

THESIS FOR THE DEGREE OF DOCTOR OF PHILOSOPHY

Experimental and Modeling Studies of Sulfur-Based Reactions in
Oxy-Fuel Combustion

DANIEL FLEIG

Department of Energy and Environment
Division of Energy Technology

CHALMERS UNIVERSITY OF TECHNOLOGY

Göteborg, Sweden 2012

Experimental and Modeling Studies of Sulfur-Based Reactions in Oxy-Fuel
Combustion
DANIEL FLEIG
ISBN 978-91-7385-780-2

© DANIEL FLEIG, 2012.

Doktorsavhandlingar vid Chalmers tekniska högskola
Ny serie nr 3461
ISSN 0346-718X

Department of Energy and Environment
Division of Energy Technology
Chalmers University of Technology
SE-412 96 Göteborg
Sweden
Telephone + 46 (0)31-772 1000

Reproservice, Chalmers University of Technology
Göteborg, Sweden 2012

Experimental and Modeling Studies of Sulfur-Based Reactions in Oxy-Fuel Combustion

ABSTRACT

Oxy-fuel combustion is a technology for CO₂ capture that is suitable for large-scale, coal-fired power plants. In this system, the combustion air is replaced by a mixture of O₂ and recycled flue gases, so as to enrich for CO₂ in the flue gas. These changes in combustion conditions have impacts on the degree of corrosion and flue-gas cleaning issues. In this thesis, the chemistry of sulfur-containing compounds during oxy-fuel combustion is examined through experimental and modeling studies. Since the concentration of formed SO₃ is important for high- and low-temperature corrosion, the formation of SO₃ is studied in detail in the present work.

The formation of SO₃ was characterized experimentally under different post-flame conditions in a quartz reactor. The gas-phase chemistry was analyzed using a detailed kinetic gas-phase model. The influences of the operating conditions of the Chalmers 100-kW_{th} oxy-fuel test unit on the formation of SO₃ were investigated using C₃H₈ as the fuel and SO₂ injection into the feed gas. Different SO₃ measurement techniques were applied and compared. A sulfur mass balance was established in the Chalmers 100-kW_{th} oxy-fuel test unit during oxy-fuel and air-fired combustion with lignite as the fuel. In each test case, the quantities of sulfur in the fuel, flue gas, ash, and condensed water were determined.

Although the SO₂ emissions (mg/MJ_{fuel}) decreased, the SO₂ concentrations were several-fold higher in oxy-fuel combustion than in air-fired combustion conditions. Simultaneously, the level of sulfur self-retention by the ash was increased during oxy-coal combustion, possible due to the increased concentration of SO₂ during oxy-fuel combustion. The increased concentration of SO₂ during oxy-fuel combustion generally results in an increase in SO₃ concentration, which leads to an increased acid dew-point temperature, especially if a wet flue-gas recycle (FGR) is applied. The experiments and modeling show that SO₃ formation is favored to a greater degree in a CO₂ atmosphere than in an N₂ atmosphere. However, during the conversion of CO, the rate of SO₃ formation may be significantly reduced in a CO₂ atmosphere, as compared to formation in an N₂ atmosphere. The SO₃ formation increased with residence time, as well with the temperature in the furnace. Therefore, the formation of SO₃ is enhanced for a decrease in the FGR ratio in oxy-fuel combustion. That means that the FGR ratio and the location of flue-gas desulfurization are important design criteria with respect to SO₃ formation in an oxy-fuel power plant.

Keywords: Carbon capture and storage; oxy-fuel; sulfur; SO₂; SO₃; H₂SO₄; acid dew-point; corrosion; coal combustion; flue gas recycle

List of Publications

This thesis is based on the following five publications and one manuscript:

- I. Fleig, Daniel; Normann, Fredrik; Andersson, Klas; Johnsson, Filip; Leckner, Bo: The fate of sulphur during oxy-fuel combustion of lignite. *Energy Procedia*, 2009, 1, 383-390.
<http://www.sciencedirect.com/science/article/pii/S1876610209000538>
- II. Fleig, Daniel; Andersson, Klas; Johnsson, Filip; Leckner, Bo: Conversion of Sulfur during Pulverized Oxy-coal Combustion. *Energy & Fuels*, 2011, 25, 647-655.
<http://pubs.acs.org/doi/abs/10.1021/ef1013242>
- III. Fleig, Daniel; Andersson, Klas; Normann, Fredrik; Johnsson, Filip: SO₃ Formation under Oxyfuel Combustion Conditions. *Industrial & Engineering Chemistry Research*, 2011, 50, pp. 8505-8514.
<http://pubs.acs.org/doi/abs/10.1021/ie2005274>
- IV. Fleig, Daniel; Andersson, Klas; Johnsson, Filip: Influence of Operating Conditions on SO₃ Formation during Air and Oxy-Fuel Combustion. *Industrial & Engineering Chemistry Research*, 2012, 51, pp. 9483–9491.
<http://pubs.acs.org/doi/abs/10.1021/ie301303c>
- V. Fleig, Daniel; Vainio Emil; Andersson, Klas; Brink Anders; Johnsson, Filip; Hupa Mikko: Evaluation of SO₃ Measurement Techniques in Air and Oxy-Fuel Combustion. *Energy & Fuels*, 2012, 26, pp. 5537–5549.
<http://pubs.acs.org/doi/abs/10.1021/ef301127x>
- VI. Fleig, Daniel; Alzueta, María Uxue; Normann, Fredrik; Andersson, Klas; Johnsson, Filip: Measurement and Modeling of Sulfur Trioxide Formation in a Plug-Flow Reactor under Post-Flame Conditions (to be submitted for publication).

The author of this thesis is the principal author of each of the listed papers. The modeling work of Paper I was performed by Fredrik Normann.

Acknowledgments

I thank my supervisor Klas Andersson for his support with both theoretical and practical issues during my research work. You always took time for discussion if at all possible, which created a reliable basis for my research. I also wish to thank my supervisor Professor Filip Johnsson for his good support during my research work and for making the research possible. I thank Professor Emeritus Bo Leckner for interesting discussions and his valuable help during the writing of my academic papers.

A special thanks to Fredrik Normann for his help during my research, for his contributions as co-author of the papers, and especially for his help with the modeling work. Thank you Johannes Öhlin for technical assistance during the measurements and unit operation. Thank you Daniel Bäckström and Daniel Kühnemuth for assistance during the experiments and for good discussions. I would also like to thank our excellent research engineers, Rustan Marberg, Jessica Malene Bohwalli, and Ulf Stenman, for technical support with the measurement equipment and the Chalmers oxy-fuel unit. Inger Hessel is thanked for help with administrative issues. Thank you to Lars-Erik Åmand for explaining the FTIR instrument. Thank you Jorge Giménez-López from the University of Zaragoza for your valuable comments with respect to my modeling work.

I would like to express my gratitude to Emil Vainio and Anders Brink from Åbo Akademi for the good cooperation during our SO₃ measurement campaign. I thank Torgny Viberg from Force Technology Sweden AB for assistance with the controlled condensation measurements. I thank Professor Maria Uxue Alzueta for facilitating my stay and research at the University of Zaragoza, Aragón Institute of Engineering Research. Furthermore, I want to thank all the staff at the Aragón Institute of Engineering Research for their support during my stay in Zaragoza.

The financial support of Vattenfall AB is gratefully acknowledged.

Daniel Fleig

Göteborg, November 2012

Table of Contents

1 - Introduction.....	1
1.1 Aim and Scope.....	2
1.2 Content	3
1.3 Sulfur-Related Problems in Combustion Processes.....	3
2 - Sulfur in Coal Combustion	7
2.1 The Fate of Sulfur during Pulverized Coal Combustion	7
2.2 Increased Concentration of SO ₂ in Oxy-Coal Combustion	9
2.3 Formation of SO ₃	10
2.4 Increased Concentration of SO ₃ in Oxy-Coal Combustion	11
2.5 SO ₃ Measurement.....	12
2.6 Impacts of the Oxy-Fuel Atmosphere - Summary	13
3 - Method.....	15
3.1 SO ₃ Measurement Methods	15
3.2 Experiments in the Chalmers 100-kW _{th} Oxy-Fuel Test Unit.....	22
3.3 Plug-Flow Reactor Experiments	28
3.4 Modeling Work.....	30
4 - Results and Discussion.....	33
4.1 Gas-Phase Sulfur Chemistry in Air and Oxy-Fuel Atmospheres.....	33
4.1.1 Equilibrium Considerations for Gaseous Sulfur Species	33
4.1.2 H ₂ S Formation.....	35
4.1.3 SO ₃ Formation – Experiments and Modeling.....	36
4.1.4 Evaluation of the SO ₃ Measurement Techniques	43
4.2 Release and Conversion of Sulfur during Coal Combustion	46
4.2.1 Sulfur Release.....	46
4.2.2 The Fate of Sulfur in Oxy-Coal Combustion.....	48
5 - Conclusions.....	55
6 - References	57
Papers.....	I – VI
Appendix (Reaction Mechanism)	

1 - Introduction

At the same time as global demand for electricity is increasing, calls to reduce carbon dioxide (CO₂) emissions, as a measure to counteract global warming, are intensifying. A major proportion of the electricity generated today originates from fossil fuels, with coal as the main fuel source. In the long-term perspective, the switch from fossil fuels to renewable energy sources is unavoidable, not least due to the fact that the supply of fossil fuels is limited. Nevertheless, over the coming decades, at least up to the year 2050, meeting the electricity demand without the use of fossil fuels is unrealistic. The strategy of capture and storage of CO₂ (Carbon Capture and Storage; CCS) from power plants offers the possibility to reduce drastically CO₂ emissions with a continued use of fossil fuels. To enable CCS, CO₂ must be captured from the flue gas, as co-storage of nitrogen (N₂) is too expensive and would require too much space. The oxy-fuel combustion process is one of the most promising CO₂ capture technologies, since it is based primarily on commercial components, thus lowering the investment risks.

In oxy-fuel combustion, oxygen (O₂) is used instead of air to oxidize the fuel, so as to produce a flue gas with a high concentration of CO₂. The basic principle of oxy-fuel combustion is illustrated in Figure 1.1. A large amount of flue gas is recycled to replace the absent air-N₂, to avoid excessive combustion temperatures. The type of flue-gas recycle (FGR) method used, e.g., wet or dry and the level of O₂, is important in the management of the combustion process. In oxy-fuel combustion, the combustion takes place in an atmosphere that contains high concentrations of combustion products. If dry-FGR is applied, the combustion takes place in a CO₂-based atmosphere, whereas if wet-FGR is applied, the combustion takes place in a water (H₂O) plus CO₂-based atmosphere. This has important implications for the combustion chemistry. In this thesis, some aspects related to sulfur (S) chemistry are examined.

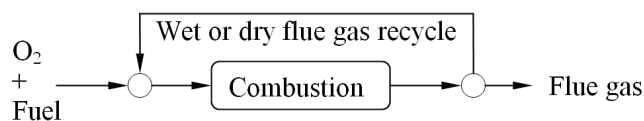


Figure 1.1 The basic principle of oxy-fuel combustion.

1.1 Aim and Scope

Since the terms and conditions for oxy-fuel combustion differ from those for air-firing, sulfur chemistry must be investigated under oxy-fuel conditions. Sulfur is involved in high-temperature corrosion (HTC) and has other undesirable effects on power plant equipment, such as low-temperature corrosion (LTC). Furthermore, the concentrations of sulfur species in the flue-gas are important with respect to flue-gas cleaning. Therefore, the overall objective of this research is to clarify the behavior of sulfur during oxy-fuel combustion. A focus of the present research is to investigate the formation of sulfur trioxide (SO_3) during oxy-fuel and air-fired combustion.

The concentration of sulfur dioxide (SO_2) during oxy-coal combustion is significantly higher than that during air-fired combustion, while the level of SO_2 emission ($\text{mg}/\text{MJ}_{\text{fuel}}$) is much lower. It is an open question as to where in the process the sulfur accumulates and therefore it is of interest to clarify the fate of sulfur in combustion facilities that operate under oxy-coal conditions. With respect to flue-gas cleaning, it is also necessary to know the amount of SO_2 that is formed during oxy-coal combustion. The concentration of SO_2 will influence the formation of SO_3 , which has a significant impact on HTC and LTC. Measurements of SO_3 in the stack gas from oxy-coal combustion reveal significantly increased concentrations of SO_3 compared to the levels from air-fired combustion. However, there are no detailed studies into the reasons behind the increase in SO_3 concentration under oxy-fuel conditions. It is necessary to clarify the rate of SO_3 formation during oxy-fuel combustion. Even for air-fired combustion, the measurements and modeling data with respect to SO_3 formation are limited, mainly because the measurement of SO_3 is problematic.

This thesis examines sulfur chemistry under air-fuel and oxy-fuel conditions. The main objective is to determine the fates of the main sulfur-containing compounds under both gas-fired and coal-fired conditions. Special attention is focused on the gas-phase sulfur chemistry in relation to coal-fired boilers. This aspect of the chemistry was studied through experiments and detailed kinetic chemistry modeling. The formation of SO_3 was identified as being of special importance for oxy-fuel combustion. In addition, there are few publications regarding the accuracy and applicability of different SO_3 measurement techniques in general and there are no experimental studies to compare different SO_3 measurement techniques in oxy-fuel combustion. Therefore, different SO_3 measurement techniques were tested in the Chalmers 100-kW_{th} oxy-fuel test unit during air-fired and oxy-fuel operation with propane (C_3H_8) as the fuel and in conjunction with the injection of SO_2 in the feed gas. The levels of formation of SO_3 during

different oxy-fuel operating conditions in the Chalmers oxy-fuel test unit were investigated in detail. The impacts of different post-flame conditions on gas-phase SO_3 formation were mapped in experiments using a quartz flow reactor. A plug-flow model combined with the detailed reaction mechanism was used for interpretation and discussion of the experimental data. A sulfur mass balance was established in the Chalmers oxy-fuel unit using lignite as the fuel, with the aims of identifying and quantifying the sulfur sinks in the unit.

1.2 Content

The present thesis consists of five Chapters, six appended papers, and an Appendix that details the applied reaction mechanism. Chapter 1 describes the aims and scope of the thesis, and outlines the sulfur-related problems that occur during coal combustion. Chapter 2 provides a brief overview of the behavior of sulfur during pulverized coal combustion. The general differences between oxy-fuel and air-fired combustion systems with respect to sulfur chemistry are identified, and previous studies in this research area are presented. The methods of the present thesis are summarized in Chapter 3, and the main results are presented and discussed in Chapter 4. Finally, the conclusions are presented in Chapter 5.

This research is based on experimental studies and is supported by modeling work, as well as data from the literature. Paper I outlines the sulfur-related issues under oxy-coal conditions and is therefore titled: “The fate of sulphur during oxy-fuel combustion of lignite”. Paper II contains the results of experiments performed in the Chalmers oxy-fuel unit that were aimed at identifying and quantifying sulfur sinks. In Paper III, the formation of SO_3 is investigated using a detailed gas-phase chemistry model for different oxy-fuel cases. Paper IV investigates experimentally the influences of operating conditions on the formation of SO_3 in the Chalmers oxy-fuel unit with C_3H_8 as the fuel and injection of SO_2 into the oxidizer. In Paper V, different SO_3 measurement techniques are evaluated during air-fired and oxy-fuel combustion processes in the Chalmers oxy-fuel unit. In Paper VI, SO_3 measurements are performed in a plug-flow reactor to determine the rate of SO_3 formation for different gas compositions in terms of dependence upon reactor temperature.

1.3 Sulfur-Related Problems in Combustion Processes

Problems associated with sulfur during coal combustion are often related to the amount of SO_3 present in the flue gases. Therefore, the extent of formation of SO_3 during combustion has important consequences for boiler operation.

However, since SO₂ is the main sulfurous oxide and SO₃ is formed *via* SO₂, the concentration of SO₂ also has relevance for efficient boiler operation. The concentration of SO₂ is also a critical process parameter for flue-gas cleaning downstream of the boiler. In this Section, sulfur-related problems associated with boiler operation in a pulverized coal combustion system are briefly discussed.

High-Temperature Corrosion (HTC)

HTC, which is also known as fire-side corrosion, was first recognized as a serious problem in the USA in 1942 when slag tap furnaces (molten slag) were used instead of dry bottom-type furnaces.¹ Subsequently, a correlation between SO₃ and HTC was identified.¹ HTC is often caused by low-melting deposits, particularly alkali salts. The alkali metal, chlorine (Cl), and sulfur contents of the fuel are critical parameters. Sulfur and chlorine compete with each other to form either alkali sulfates (Na₂SO₄ and K₂SO₄) or alkali chlorides (NaCl and KCl). The formation of alkali sulfates instead of alkali chlorides is advantageous from a corrosion point of view. Therefore, the hydrogen chloride (HCl)/SO₂ molar ratio in the flue gas is important with respect to HTC. Using equilibrium calculations, Otsuka² concluded that coals that have high concentration of Cl and S favor the formation of sulfate salts during combustion. In coal-fired boilers, HTC is also caused by complex sulfates, such as alkali iron trisulfates [K₃Fe(SO₄)₃ and Na₃Fe(SO₄)₃], which are formed from alkali sulfates and SO₃.¹⁻⁴ Corrosive liquid pyrosulfates (Na₂S₂O₇ and K₂S₂O₇), which are formed from alkali sulfates and SO₃, may also be important at lower temperatures (e.g., wall tubes).^{1,4} Elevated concentrations of SO₂ and SO₃ in oxy-fuel combustion may increase the formation of alkali sulfates.⁵ At the same time, compared to air-fired conditions, oxy-fuel combustion with a wet flue-gas recycle process is expected to result in a higher concentration of Cl. In summary, there is a risk that coals that have a weak potential for inducing corrosion under air-fired conditions have a greater potential for corrosion under oxy-fuel conditions. Therefore, it is of interest to investigate the chemistry of sulfur in oxy-fuel combustion processes.

Low-Temperature Corrosion (LTC)

During cooling of the flue gas, SO₃ starts to combine with H₂O at temperatures <500°C, to form gaseous sulfuric acid (H₂SO₄):^{6,7}



At temperatures <200°C, almost all the SO₃ is converted to H₂SO₄.⁷ Thus, discussions of SO₃ in relation to flue-gas measurements generally refer to the

measurement of gaseous H_2SO_4 , and this is also the case in the present study. Gaseous H_2SO_4 combines with H_2O at points below the acid dew-point, which represents the temperature and pressure at which acid condensation is initiated. This can result in LTC due to the formation of liquid films on metal surfaces or the accumulation of small corrosive drops on equipment surfaces. The acid is highly corrosive and typically contains more than 70 mole% H_2SO_4 (see Land⁸). Figure 1.2 illustrates the influence of the H_2SO_4 (g) partial pressure in the flue gas on the acid dew-point temperature for different H_2O (g) partial pressures. In oxy-fuel combustion with a wet recycle, the H_2O concentration will be several-fold higher than the H_2O concentration during air-fired combustion, which means that the acid dew-point temperature is higher in oxy-fuel combustion with a wet recycle than in an air-fired combustion system.⁹

The involvement of SO_3 in LTC of air-heater and economizer surfaces is well-documented.¹⁰⁻¹³ LTC can be controlled either by operating above the acid dew-point temperature, with the drawback that the efficiency of the unit may be reduced, or using acid-resistant steels in the low-temperature region, in which entails higher investment costs. SO_3 can cause further problems at the cold end, such as reduced mercury removal, air preheater fouling, and plugging of the SCR catalyst by formed ammonium sulfates.¹⁴⁻¹⁶

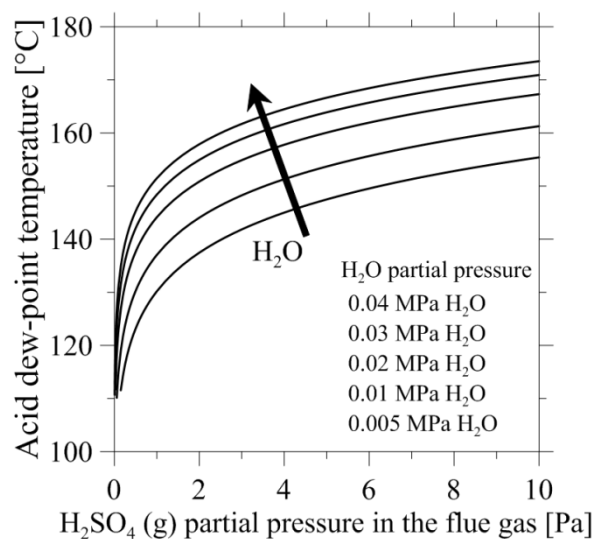


Figure 1.2 Acid dew-point temperature versus H_2SO_4 (g) partial pressure for different H_2O (g) pressures in the flue-gas (adapted from Verhoff and Banchemo¹⁷).

Environmental Problems and Measures

Sulfur oxides are harmful to both human health and the natural environment, not least due to the formation of sulfurous and sulfuric acid, as well as smog. Sulfur oxides are responsible for acid rain, leading to soil and water acidification and acidic damage to plants and buildings.

In response to high levels of sulfur compound generation in parts of England, flue-gas desulfurization (FGD) units were installed during the 1930s to minimize SO_x emissions from power plants, although their wide-scale implementation was not until the 1970s, as part of governmental decisions and regulations to reduce SO_x emissions.¹⁸ Global anthropogenic sulfur emissions therefore peaked in the early 1970s and decreased until 2000, mainly as result of using FGD units and switching to fuels with lower sulfur contents in Europe and North America. However, since the turn of the century, sulfur emissions have increased once more due to higher emission levels in China and other developing countries.¹⁹

SO_3 emissions in the stack gas from coal-fired plants constitute the so-called “blue plume”. Blue plume is caused by aerosol formation from gaseous H_2SO_4 during the cooling of the flue-gas, leading to a typically blue or brown-orange coloration of the stack gas.²⁰ The complete removal of such aerosols before the stack is difficult to achieve through wet-FGD.²¹

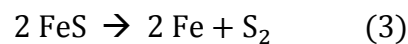
In the oxy-fuel combustion process, apart from conventional flue-gas cleaning equipment, new opportunities are presented, since the CO_2 has to be liquefied. Therefore, oxy-fuel combustion offers good possibilities to reduce further SO_x emissions, in comparison to conventional air-fired power plants. While the co-storage of SO_x has also been proposed, owing to acid formation and the potential formation of calcium sulfate, specific storage field conditions have to be considered as well.

2 - Sulfur in Coal Combustion

2.1 The Fate of Sulfur during Pulverized Coal Combustion

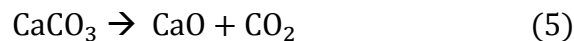
The level of sulfur in the flue gas from pulverized coal combustion is primarily dependent upon the type of coal used, as the sulfur content and the ways in which sulfur and ash-forming matter are bound differ among coal types. The sulfur content of coals varies from 0.1% to 11% per mass.^{22,23} For high-sulfur coals, desulfurization before combustion can be applied, although this is not the norm and usually the sulfur content is <4 wt. %.

The main sulfur reaction routes during pulverized coal combustion are summarized in Figure 2.1 and explained in this Section. The sulfur in coal can be bound as sulfides, organic sulfur compounds, sulfates, and traces of elemental sulfur.²⁴ Sulfides and organic sulfur compounds are generally the main sulfur-containing species in coals, whereas the levels of sulfates and elemental sulfur are usually low.^{22,23} During devolatilization, most of the organic sulfur compounds and approximately half of the sulfides are released to the gas-phase. Sulfur is released from sulfates only during char combustion.²⁵ Pyrite (FeS_2), which usually comprises a major fraction of sulfides in coal, is released according to the following reactions:²⁶

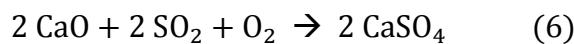


Reaction 2 occurs mainly during devolatilization, and Reaction 3 occurs during char combustion. SO_2 is formed by Reaction 4 and is the thermodynamically favored gaseous sulfur compound at high temperatures ($>1000^\circ\text{C}$) when O_2 is present in excess.^{27,28} In sub-stoichiometric (fuel-rich) regions, significant concentrations of hydrogen sulfide (H_2S) can occur.^{27,28} H_2S is released from organic sulfur compounds in the coal and SO_2 can be further converted to H_2S under sub-stoichiometric conditions, which is especially relevant for oxy-coal combustion, where the feed-gas (oxidizer) contains SO_2 .

However, not all the sulfur in the coal is released to the gas-phase; a portion remains unburnt, together with the ash-forming matter. Furthermore, not all the sulfur released to the gas-phase remains there as SO_x , since SO_x can react with alkaline earth metals and alkali metals to form sulfates.^{22,29-31} Alkaline earth metals and alkali metals are commonly found in coals, although their contents and reactivities vary significantly among different coals. The capture of sulfur by ash-forming matter, termed ‘sulfur self-retention by ash’, depends mainly on fuel-specific characteristics, such as coal particle size, and the ways in which sulfur, alkali metals, and alkaline earth metals are bound.³² Calcium (Ca) plays a dominant role in sulfur self-retention by ash and, consequently, the Ca/S molar ratio of coal is an important factor.^{30,32} Calcium in coals appears as calcite (CaCO_3 , common in coals³³), dolomite [$\text{CaMg}(\text{CO}_3)_2$], organic Ca, and Ca in clays and silicates. CaCO_3 is converted to lime (CaO) during combustion when the temperature is sufficiently high and the CO_2 partial pressure is sufficiently low, in accordance with:



The CaO initially formed from CaCO_3 (or dolomite or organic Ca) has a highly porous structure and reacts readily with SO_2 to form CaSO_4 :



However, at the high temperatures present during pulverized-coal combustion, the CaO particles can sinter, and thereby lose reactivity. Additional CaSO_4 formation fills the pores and reduces the theoretical sulfation potential of the CaO particles. Therefore, given the high temperatures during pulverized coal combustion, the addition of lime can never be as effective as it is during circulating fluidized bed (CFB) combustion.

In oxy-fuel combustion, H_2O is removed from the flue gas and a small fraction of the SO_x in the flue gas is absorbed by the condensate formed in the flue-gas condenser.³⁴ This phenomenon is indicated in Figure 2.1, although it should be noted that this is not part of the combustion process.

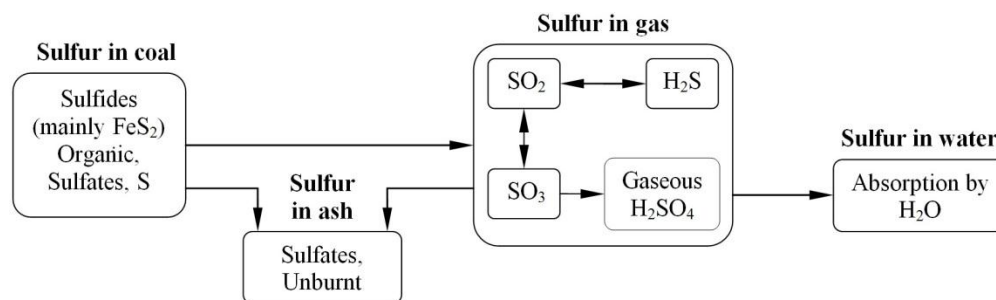


Figure 2.1 Reactions of sulfur during oxy-coal combustion (Paper I).

2.2 Increased Concentration of SO₂ in Oxy-Coal Combustion

In oxy-coal combustion, the level of SO₂ emission (mg/MJ_{fuel}) is significantly lower than in air-fired combustion. However, due to the absence of airborne N₂, the concentration of SO₂ is significantly increased, as demonstrated by several experimental studies.³⁴⁻⁴¹ Most of these studies investigated only the gas phase, and it remains an open question as to where in the process the sulfur is retained. Kiga and Takano³⁷ measured the mass flow of sulfur in the ashes, although their sulfur mass balance was not completely closed. Stanger and Wall⁴⁰ reported significantly reduced SO₂ emissions under oxy-coal conditions, as compared with air-fired conditions, albeit without any major differences in the sulfur contents of the ashes. Without providing the experimental data related to the deposits, they stated that the missing sulfur in oxy-fuel combustion might be the result of a higher rate of deposition of sulfur-containing compounds, as compared with air-fired combustion. Since there the only significant sulfur sink is the ash, the ash and deposits formed under oxy-fuel conditions should contain more sulfur than those formed under air-fired conditions (as discussed in Paper II).

The higher concentration of SO₂ associated with oxy-coal combustion generally favors sulfation and stabilization of the formed sulfates.⁴²⁻⁴⁴ Moreover, the conditions for sulfate formation are enhanced by the high concentration of CO₂ during oxy-fuel combustion, which leads to an increase in the calcination time for CaCO₃ particles, as compared with air-fired combustion. (Such considerations are only relevant for coals in which most of the Ca is bound as CaCO₃ or for combustion units in which limestone is added.) Since the calcination of CaCO₃ particles occurs more slowly in a CO₂-rich environment, calcination occurs more concomitantly with sulfation, in contrast to the situation of an N₂-rich environment in which the CO₂ produced during calcination causes the developing CaSO₄ layer to be more porous and brittle.⁴⁵ Thus, the desulfurization efficiency of limestone in a CO₂/O₂ atmosphere at 1200°C was found to be higher than the desulfurization efficiency of limestone in an air-combustion atmosphere at 900°C (3-sec residence time).⁴⁵ Chen et al.⁴⁵ further demonstrated that the optimal desulfurization temperature of limestone is higher in a CO₂/O₂ atmosphere (1050°C) than in air (900°C). Furthermore, CaO, calcinated in a CO₂/O₂ environment, has a smaller specific surface area but larger pore diameter than CaO calcinated in air, which increases its sulfation efficiency due to reduced pore filling and plugging.⁴⁶ Therefore, the efficiency of desulfurization can be significantly higher in oxy-fuel combustion than in air-fired combustion.

The CO₂ partial pressure also governs the temperature at which calcination (Reaction 5) occurs.^{47,48} The higher concentration of CO₂ in oxy-fuel combustion raises the lower temperature limit for calcination to around 900°C, as compared

with approximately 800°C in air-fired combustion (atmospheric conditions). Therefore, calcination does not take place at temperatures <900°C in oxy-fuel combustion owing to the high partial pressure of CO₂, which favors the direct sulfation of CaCO₃ (similar to the situation in pressurized air-fired combustion):



This reaction is important for oxy-fuel CFB combustion because the temperatures therein are <900°C. However, in pulverized oxy-coal combustion, the temperature is sufficiently high for CaO to be formed.

2.3 Formation of SO₃

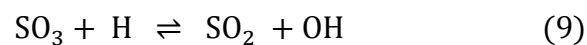
The equilibrium calculations for typical flame conditions show that, under O₂-rich conditions, the only noteworthy sulfurous species formed are SO₂, together with small amounts of SO₃ and sulfur oxide (SO), whereas under fuel-rich conditions, the amount of formed SO₃ is insignificant.^{27,28} However, at lower temperatures, the equilibrium shifts towards SO₃, although SO₃ formation is kinetically controlled and the SO₃/SO_x conversion ratio for coal combustion is usually <4% (see Paper III).

Hindiyarti et al.⁴⁹ identified the following four reactions as being important for gas-phase SO₃ formation in combustion-relevant systems, as confirmed in Paper III:

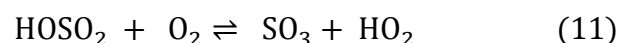
primary oxidation of SO₂,



reduction of SO₃ by H-radicals,



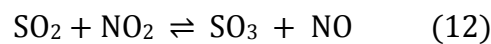
and secondary formation of SO₃ *via* HOSO₂,



However, SO₃ may be consumed by the reverse of Reactions 11 and 10 when the level of radicals is high.⁴⁹ The primary formation of SO₃ (Reaction 8) is most important at high temperatures (>1150 K), whereas secondary formation of SO₃ (Reaction 11) is more pronounced at moderate temperatures (1000–1200 K) (Paper III).

Since SO₃ formation decreases in line with decreasing temperature, the cooling rate of the flue gas governs SO₃ formation.¹⁴ Furthermore, the formation of SO₃ is heavily dependent upon the concentrations of SO₂ and O₂.⁵⁰ Therefore, excess O₂ is usually restricted in oil-fired boilers to minimize SO₃ formation (0.3%–0.5% excess O₂).^{50,51} The concentration of SO₂ depends on the sulfur content of the coal and the extent of sulfur self-retention by the ash. However, SO₃ may also participate in heterogeneous reactions.^{14,52} For example, the formation of SO₃ is favored by fly ash that contains iron oxide (Fe₂O₃)^{29,52-54} or vanadium pentoxide (V₂O₅)^{53,55}, whereas if the alkalinity of the ash is high, it may capture the SO₃.⁵⁰

Reactions between NO_x and SO_x species^{6,56,57}, such as



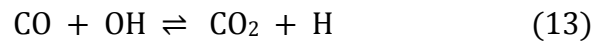
may influence SO₃ formation, although these reactions remain controversial⁵⁸. Wendt et al.⁵⁷ estimated that SO₃ formation, as a result of such reactions, amounted to 0.01 ppm SO₃ for cooling of the flue gas from 1800 K to 600 K in 2 seconds (initial conditions: 3% O₂; 1000 ppm SO₂; and 500 ppm NO). This implies that the impacts of direct NO_x and SO_x interactions are of less importance for SO₃ formation in combustion processes.

2.4 Increased Concentration of SO₃ in Oxy-Coal Combustion

Measurements performed under oxy-coal conditions reveal a concentration of SO₃ that is several times higher than that seen under air-fired conditions.^{38-41,59-61} Most of the results are based on measuring the SO₃ concentration in the stack gas. However, Eddings et al.⁶¹ measured SO₃ concentrations by extracting flue gas at higher temperatures (from 800 K to 1300 K). A detailed overview of the results of the SO₃ measurements under oxy-fuel conditions, as compared to air-fired conditions, is provided in Paper III (page 8509). Comparing the available data, it is clear that coal types with a Ca-rich ash have the lowest SO₃ concentrations in the stack. The data also demonstrate that higher concentrations of SO₂ lead to higher concentrations of SO₃. However, it is unclear as to which other factors influence the amount of SO₃ formed in oxy-fuel combustion. There is a need to clarify SO₃ formation in oxy-fuel combustion using a more general approach. Therefore, in this summary and especially in Papers III, IV, and VI, the influences of altered combustion conditions on SO₃ formation are discussed in detail.

With regard to SO₃ formation, there are two main differences between oxy-fuel combustion and air-fired combustion. First, the concentration of SO₂ increases in oxy-fuel combustion, and this has a strong impact on the concentration of SO₃. Second, combustion takes place in an atmosphere with a high CO₂ concentration

and, depending on recycling conditions, possibly a high H₂O concentration, which has an impact on the concentrations of radicals. Liu et al.⁶² and Glarborg et al.⁶³ concluded that the reaction



can be reversed in an oxy-fuel flame, thereby consuming H-radicals. This reduces the size of the O-/H-radical pool, as Reaction 13 then competes with Reaction 14:



This results in slower oxidation of the fuel under oxy-fuel conditions, as compared with air-fired conditions, assuming that the other conditions (temperature, O₂ concentrations) are comparable. However, in the burnout zone, Reaction 13 is no longer reversed and H-radicals are produced. In the present thesis, the impact of a CO₂ atmosphere on SO₃ formation is investigated through experimental and modeling studies.

2.5 SO₃ Measurement

While there are several methods for analyzing the SO₃ concentration in flue gases, few experimental studies have been conducted to compare different SO₃ measurement techniques, with the only detailed study having been performed by Cooper et al.⁶⁴⁻⁶⁶ No experimental study has been undertaken to date to compare different methods for measuring SO₃ during oxy-fuel combustion. Therefore, the present work involved the evaluation of different methods for SO₃ measurement during air-fired and oxy-fuel combustion.

As SO₃ is a strongly reactive gas, measurements of SO₃ are difficult. More specifically, the analysis of SO₃ in flue gases may be hindered by: 1) comparatively low concentrations of SO₃; 2) high concentrations of SO₂, which constitute an interference factor; 3) oxidation of SO₂ to SO₃ by catalytically active substances, such as iron oxides (fly ash particles) in the measurement line; 4) the fact that SO₃ starts to form gaseous H₂SO₄ at temperatures <500°C; 5) the removal of SO₃/H₂SO₄ by the particle filter, when extractive techniques are used, with the consequence that the detected SO₃ concentration is too low^{67,68}; and 6) the fact that SO₃/H₂SO₄ is very reactive and can be lost due to surface reactions before it reaches the measurement cell, despite the temperature being above the acid dew-point.^{66,68}

2.6 Impacts of the Oxy-Fuel Atmosphere - Summary

Table 2.1 summarizes the impacts of the oxy-fuel combustion conditions on the sulfur chemistry discussed above.

Table 2.1 Impacts of the oxy-fuel combustion conditions on the sulfur chemistry.

Change	Consequence
Absence of airborne N ₂	Increase in SO ₂ concentration
Increase in SO ₂ concentration	Increase in SO ₃ concentration; Improved sulfation (Paper II-IV)
Increases in concentrations of combustion products	Change in radical pool size; Improved calcination/sulfation
Change in flue gas residence time (depending on FGR ratio)	For longer residence time: increase in SO ₃ concentration (Paper III) For shorter residence time: decrease in SO ₃ concentration (Paper III)
Change in temperature conditions (mainly dependent upon the O ₂ concentration in the oxidizer)	Probably influences the release of sulfur from the coal and the capture of SO _x by ash-forming matter Influences the level of SO ₃ formation (Paper V)

3 - Method

The applied methodologies are specified in detail in each paper. A summary is provided here.

3.1 SO₃ Measurement Methods

This Section provides a summary and discussion of the SO₃ measurement techniques applied in the present work. Those include: 1. Controlled condensation method (British Standard BS 1756-4:1977); 2. Isopropanol absorption bottle method (based on EPA Method 8); 3. Salt method^{64-66,69,70}; 4. Pentol SO₃ monitor^{71,72} (first-generation system described by Jackson et al.⁷³); and 5. Acid dew-point monitor⁸.

The controlled condensation method was used as the standard for comparisons, and was applied for SO₃ measurement in Papers IV–VI, whereas the other SO₃ measurement methods were evaluated in Paper V in experiments using the Chalmers oxy-fuel unit. Methods 2, 3, and 5 were studied in cooperation with Emil Vainio and Anders Brink (Åbo Akademi, Turku, Finland). Methods 1–4 are based on chemical sorption of SO₃ followed by sulfate (SO₄²⁻) analysis after gas sampling. Methods 1–3 are extractive, and a time-averaged SO₃ concentration is measured. Method 4 is also extractive but the sulfate analysis takes place continuously. Figure 3.1 shows the principle of the sampling system that was used for chemical sorption Methods 1–4. Flue gas is extracted with a heated probe, SO₃ is absorbed downstream, and the flue-gas flow is measured. The different SO₃ measurement methods are described in detail below.

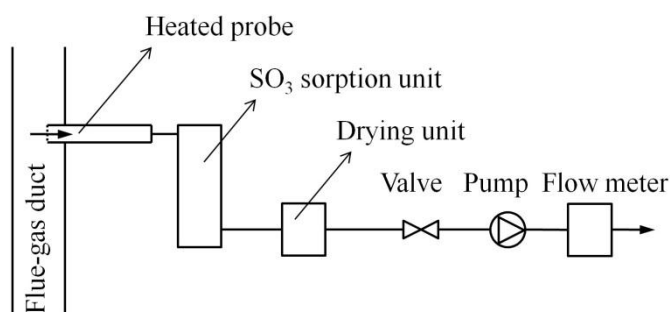


Figure 3.1 An illustration of the sampling system used in the chemical sorption methods.

Controlled Condensation Method

The controlled condensation method, which is a widely accepted and used method for SO_3 measurement, is often conducted according to the British Standard BS 1756-4:1977 and the American Standard D 3226-73T. However, both standards have been withdrawn and may be reworked. In the present work, a controlled condensation method (Figure 3.2) based on British Standard BS 1756-4:1977 was used. The method is described in detail in the Värmeforsk Handbook of Measurement⁷⁴. The principle of the controlled condensation method is to cool down the extracted flue gas to a temperature that lies between its acid dew-point and water dew-point. Thus, H_2SO_4 condensates and is adsorbed onto the condenser walls and the sintered glass filter of the glass cooler.

A flue-gas sampling time of 30 min was chosen for the measurement of SO_3 with the controlled condensation method. After gas sampling, the glass cooler was flushed with 5 vol.% isopropanol [$\text{CH}_3\text{CH}(\text{OH})\text{CH}_3$] solution. Thereafter, the amount of sulfate in the solution was determined by ion chromatography or titration, as recommended by Värmeforsk.⁷⁴ The temperature in the adsorption column (glass cooler) was maintained at between 80°C and 90°C in a water-bath. According to Cooper et al.⁶⁶, the controlled condensation method gives comparatively true results, and it is recommended by Värmeforsk⁷⁴. Maddalone et al.⁷⁵ recovered with the controlled condensation method 95% of the H_2SO_4 content of a synthetic flue gas with a coefficient of variance of $\pm 6.7\%$, which is an acceptable result in terms of accuracy and repeatability. However, Dene et al.⁶⁸ observed that the measured concentration of SO_3 could be too low because the sulfate could become trapped in the filter. Koebel et al.⁷⁶ observed that the measured SO_3 concentration might be underestimated, as complete condensation of sulfuric acid vapor is difficult to achieve.

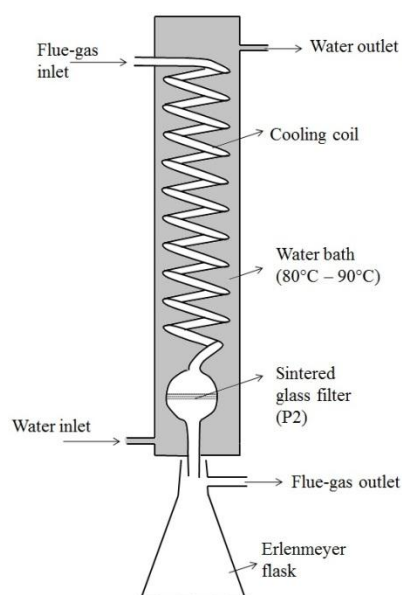


Figure 3.2 Schematic of the controlled condensation method.

Isopropanol Absorption Bottle Method

Figure 3.3 shows the setup for the isopropanol absorption bottle method applied in the present work. The method is based on EPA Method 8, with some modifications. Flue-gas was first bubbled through one impinger filled with 80 vol.% isopropanol to absorb SO_3 , and then through two impingers filled with 3 vol.% hydrogen peroxide (H_2O_2) to absorb SO_2 .

The sulfate concentration in the isopropanol solution was analyzed by the addition of thorin ($\text{C}_{16}\text{H}_{11}\text{AsN}_2\text{O}_{10}\text{S}_2$) as an indicator and titration with barium perchlorate [$\text{Ba}(\text{ClO}_4)_2$] until the color changed from yellow to light-red. Cooper et al.⁶⁶ used ion chromatography to measure the sulfate concentration in the isopropanol solution but the measured SO_3 concentration was far too high. The reason for this was slow oxidation from sulfite (SO_3^{2-}) to sulfate of the SO_2 dissolved in the isopropanol solution. The determination of sulfate content in the isopropanol solution using ion chromatography was therefore not recommended by Koebel and Elsener⁷⁶, as it normally takes too long to get the sample to a laboratory. Cooper et al.⁶⁶ reported that the dissolved SO_2 in the isopropanol solution could be removed by the bubbling of air through the solution after gas sampling. However, Koebel and Elsener⁷⁶ noted that the elimination of all SO_2 from the solution was difficult to achieve, especially if the pH value was too high, for instance due to low concentrations of SO_3 and NO_x or if ammonia (NH_3) was present.

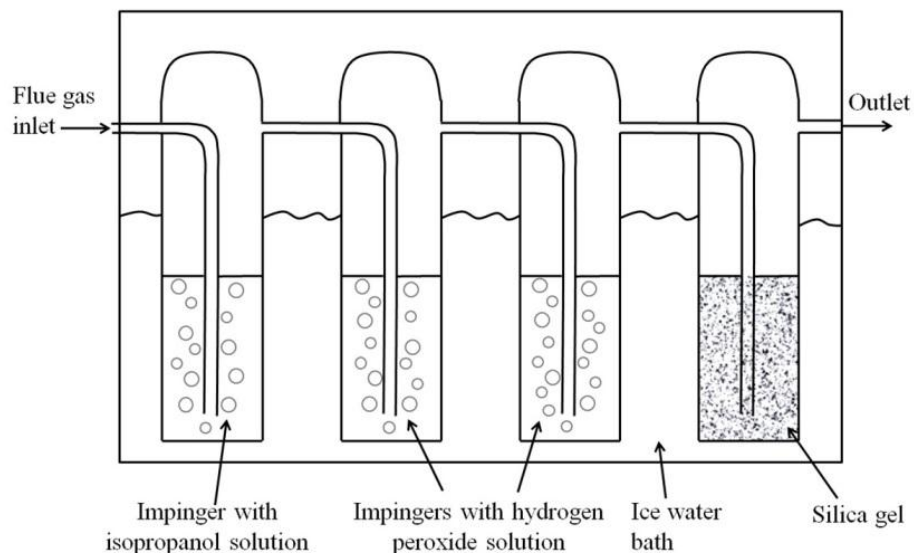


Figure 3.3. The isopropanol absorption bottle method (Paper V).

Salt Method

The principle of the salt method is that SO_3 (gaseous H_2SO_4) reacts with sodium chloride (NaCl), resulting in the formation of sodium sulfate (Na_2SO_4) and sodium bisulfate (NaHSO_4):



The salt method, which is not commonly used, was first described by Kel'man⁶⁹, later used by Roiter et al.⁷⁰, and more recently evaluated by Cooper et al.⁶⁴⁻⁶⁶ Cooper et al.⁶⁶ tested two different setups. The first comprised three or four connected-in-series, NaCl -impregnated quartz filter tubes, while the second consisted of a cheaper and simpler glass tube filled with quartz wool and NaCl . The amount of formed sulfate was detected by ion chromatography. The detected concentration of SO_3 was underestimated when using the NaCl -impregnated quartz filter tubes, and Cooper et al.⁶⁶ assumed that the amount of NaCl was too low or that the residence time was too short. However, when the simple glass tube was used, the determined concentrations of SO_3 corresponded to the results of the controlled condensation method.

The salt method was studied intensively during the SO_3 measurement campaign with the Chalmers oxy-fuel unit. A simple setup was used (Figure 3.4). Ultra-clean NaCl (~1 g) was tightly packed in a Teflon tube with an inner diameter of 8 mm. The salt was positioned using glass wool at each end of the tube. The level of SO_2 was determined simultaneously by bubbling the flue gas through two impingers with 3 vol.% H_2O_2 placed in an ice water bath. After gas sampling, the salt was dissolved in distilled deionized water and the amount of sulfate in the water was determined by ion chromatography.

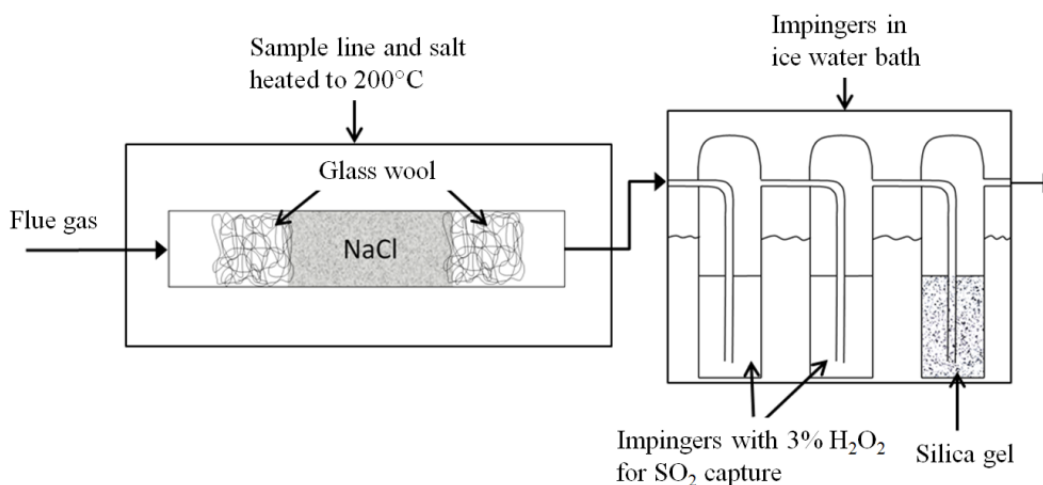


Figure 3.4. Setup of the salt method for measuring SO_3 in flue gases (Paper V).

Pentol SO₃ Monitor

The Pentol SO₃ monitor⁷¹⁻⁷³ (earlier termed the ‘Severn Science reactive gas analyser’) uses a principle similar to that of the isopropanol drop method (German Standard VDI 2462, withdrawn), although it was developed for continuous measurements of SO₃ in flue gases. Figure 3.5 illustrates the principle of the isopropanol drop method. An isopropanol solution drops in the extracted flue-gas stream and SO₃ is absorbed. After sampling, the sulfate concentration in the isopropanol solution can be analyzed by titration. The titration step is automated and takes place quasi-continuously in the Pentol SO₃ monitor.

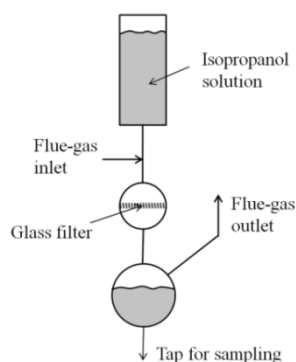


Figure 3.5. Schematic of the absorption equipment for the isopropanol drop method (Paper V).

In the Pentol SO₃ monitor, SO₃ is absorbed in a flow of 80 vol.% isopropanol directly downstream of the heated probe in a simple mixing chamber. The isopropanol flow is treated continuously with barium chloranilate (BaC₆O₄Cl₂) and the following reaction occurs:



The acid chloranilate ion absorbs light with an absorption peak at 535 nm.⁷³ The light absorption is measured in a photometer and depends on the number of chloranilate ions in the solution. The higher the absorption value, the more sulfate is present in the solution. The concentration of sulfate in the solution is proportional to the concentration of SO₃ in the flue gas.

Blauenstein⁷² and Jackson et al.⁷³ have claimed that there is no interference by SO₂ when the SO₃ monitor is used. Dene et al.⁶⁸ have confirmed that this instrument provides credible results, albeit only in the hands of a skilled operator (see Fernando⁵⁰). However, Cooper⁶⁴ measured significantly higher concentrations of SO₃ (25-fold higher on average) using the SO₃ monitor compared to the controlled condensation method. This discrepancy may be due to oxidation of the SO₂ dissolved in the isopropanol solution. It should be mentioned that the SO₃/SO_x ratio was low in this instance.

During the performance of the SO₃ measurements in the Chalmers oxy-fuel unit (Paper V), the mass flow controller of the SO₃ monitor, which measures the extracted flue-gas flow, had to be adapted for oxy-fuel operation owing to the high concentration of CO₂ in the flue gas from the oxy-fuel combustion. For oxy-fuel operation, a correction factor of 0.76 (see Brooks Instruments⁷⁷) was used. Therefore, the SO₃ concentration value displayed by the Pentol SO₃ monitor was divided by 0.76.

Acid Dew-Point Temperature Measurement

The acid dew-point temperature can be measured in a flue-gas stream by the insertion of a probe with a controllable surface temperature.^{8,78-80} After insertion, the surface temperature of the probe is decreased continuously. As soon as sulfuric acid condenses on the probe, the two electrodes generate a signal, and the acid dew-point temperature is obtained. If the H₂O content of the flue gas is known, the concentration of SO₃ can be calculated from the acid dew-point temperature (see Figure 1.2). However, the SO₃ concentration is very sensitive to the acid dew-point temperature, i.e., a small measurement error in the acid dew-point temperature results in a significant error with regard to the SO₃ concentration. Koebel et al.⁷⁶ have pointed out that the true dew-point temperature and the surface temperature of the probe are different. This difference is greater for low concentrations of SO₃ than for high concentrations of SO₃.

In the present study, an acid dew-point temperature monitor (ADM 220) from Land Instruments^{8,81} was used to measure the acid dew-point temperature of the flue gas. The probe has a sensor in the tip that consists of two platinum electrodes insulated from each other with Pyrex glass. A schematic of the probe tip is shown in Figure 3.6.

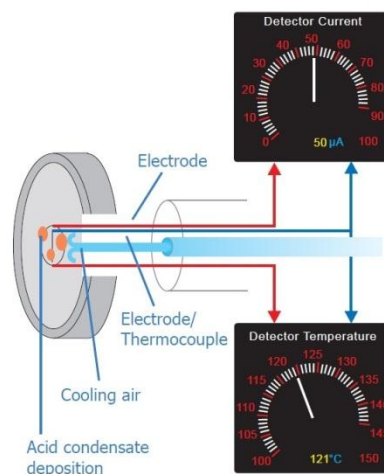


Figure 3.6 Probe tip of the acid dew-point temperature monitor (source: Land Instruments⁸¹).

The probe tip is inserted into the flue-gas channel. After the surface temperature of the sensor reaches the flue-gas temperature, the surface temperature is slowly decreased by increasing the cooling air flow. The dew-point meter shows a current of 0 μA as long as there is no condensation on the sensor surface. According to Land⁸, the acid dew-point temperature is reached when the rates of evaporation and deposition on the sensor surface are equal. This leads to a constant conductivity and Land⁸ recommends a stable current reading of around 100 μA , whereas Stuart⁷⁸ lists a stable current reading of around 50 μA . However, since in the present thesis a reading of either 50 μA or 100 μA resulted in acid-dew point temperatures that were too low, a stable current reading of approximately 1 μA was adopted.

3.2 Experiments in the Chalmers 100-kW_{th} Oxy-Fuel Test Unit

Most of the experimental work of this thesis was performed in the Chalmers 100-kW_{th} oxy-fuel test unit. Figure 3.7 shows a schematic and Figure 3.8 photos of the Chalmers oxy-fuel test unit. The flue-gas measurement positions are indicated as M1 to M15. The unit is equipped with either a top-fired pulverized coal burner or a gas burner, and it can be operated under conventional air-fired or oxy-fuel conditions with dry and wet flue-gas recycling. The process is monitored by on-line flue-gas analysis and temperature measurements in the flue gas duct and recycle loop. The volume flow of the oxidizer and the mass flow of the fuel are also continuously measured. For further information about the Chalmers test unit, see Paper II, Paper IV, and Andersson et al.⁸².

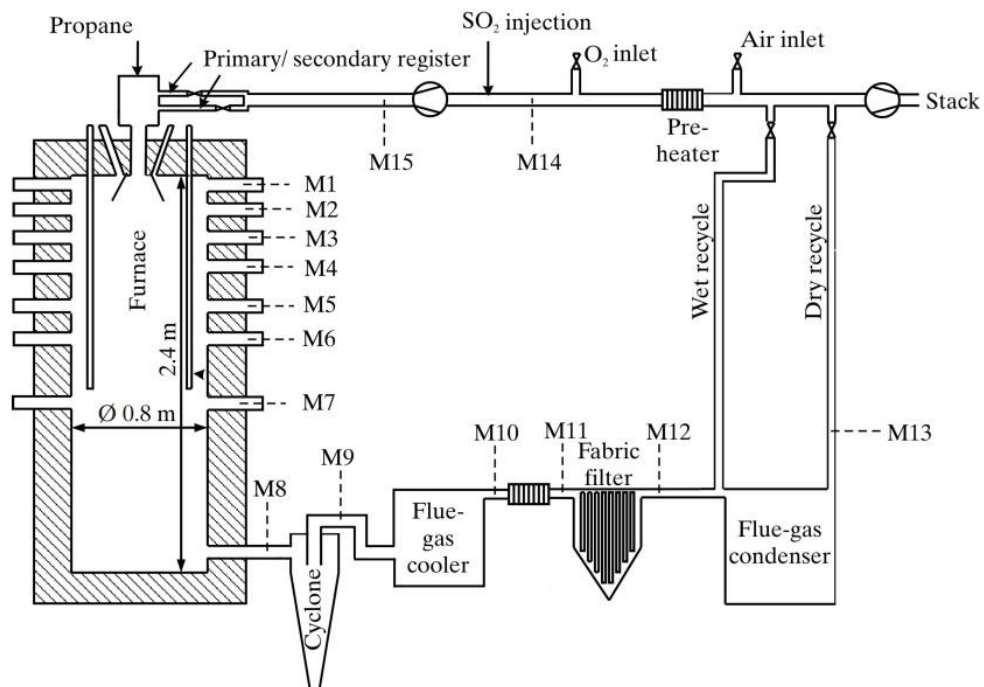


Figure 3.7 Schematic of the Chalmers 100-kW_{th} oxy-fuel test unit. Letters (M) denote measurement positions.

a)



b)



c)



Figure 3.8 Photographs of the Chalmers 100-kW_{th} oxy-fuel test unit: a) rear view; b) front view; and c) furnace with measurement ports M1 to M5.

Coal-Fired Experiments

Experiments were performed with air-fired and oxy-fuel combustion using lignite as the fuel, with the aim of studying the fate of the sulfur through composition measurements of the gases, solids, and condensate. Average proximate and ultimate analyses of the lignite are presented in Table 3.1.

Table 3.1 Proximate and ultimate analyses of the lignite (average values).

Proximate [wt.%, as received]			Volatiles [wt.%, d.a.f. ^a]	Ultimate [wt.%, d.a.f. ^a]				
$Y_{moisture}$	Y_{ash}	$Y_{combustibles}$		Y_C	Y_H	Y_N	Y_S	Y_O^b
10.6	4.56	84.8	59.2	67.0	5.37	0.83	0.89	25.9

^a Dry ash free; ^b by difference

Four different test cases were investigated (Paper II): 1) air-fired; 2) oxy-fuel with wet recycling and an O₂ feed-gas concentration of 42.6% on a dry basis (referred to as ‘OF43w’); and 3 and 4) oxy-fuel cases with dry recycle with O₂ feed-gas concentrations on a dry basis of 34.9% and 29.7%, respectively, hereinafter referred to as ‘OF35’ and ‘OF30’, respectively. The performed measurements included ash and water analyses coupled with on-line gas composition measurements upstream of the flue-gas condenser at M12 (flue gas) and, in the oxy-fuel cases, also downstream of the O₂ mixing point at M15 (feed gas). The points of measurement are shown in Figure 3.7. The measured flue-gas compositions (SO₂, O₂, and CO₂) are presented in Table 3.2 and represent the mean concentrations of the sampling sequences, which were typically 10 to 20 minutes in duration. The fuel mass flow was 13 kg/h in all the test cases, which is equivalent to a heat input of 76 kW.

Table 3.2 Experimental conditions in the test cases.

Test case	Test duration [h]	O ₂ in feed gas [vol.%, dry]	Measured flue-gas concentrations (on dry basis)		
			X _{CO2} [%]	X _{O2} [%]	X _{SO2} [ppm]
Air-fired	9.1	21	16.0	3.3	550
OF35	9.6	34.9	90.9	6.9	1870
OF43w	11.5	42.6	90.8	7.3	1955
OF30	11.0	29.7	91.4	5.7	1917

Since the overall sulfur mass balance of the system was of interest, the sulfur fractions in the ashes and water (condensate) were measured, and the amount of sulfur in the flue gas was estimated by measuring the concentration of SO₂. The total conversion of coal sulfur to SO₂ (C_{SO2}) was determined using the ratio of the measured molar fraction of SO₂ (X_{SO2, flue-gas}) in the flue gas to the maximal theoretical molar fraction if all the coal sulfur were converted to SO₂ (X_{SO2, max}).

$$C_{SO2} = \frac{X_{SO2, flue-gas}}{X_{SO2, max}} \quad (\alpha)$$

In addition, the SO_2 concentration was measured before and after passage through each component (furnace, cyclone, flue-gas cooler, fabric filter, and condenser), to identify sulfur sinks within the system. The sulfur content of the ash was determined at each location (furnace bottom, cyclone ash container, flue-gas cooler, and fabric filter). Since the sulfur content of the ash differed between locations, it was necessary to estimate the ash quantity at each location. The bottom and cyclone ashes were weighed. The ashes that were not quantified within the system, e.g., ashes found in the flue-gas cooler, fabric filter, reactor tubes, and on the walls, were treated as residual ash and calculated from the difference between the weighed ashes (bottom and cyclone ashes) and the ash content in the fuel (obtained from the fuel analysis). In addition, the elemental composition and the particle size distribution in the ashes and fuel were analyzed.

Gas-Fired Experiments

Tests were performed during air-fired and oxy-fuel combustion with C_3H_8 as the fuel and with the injection of SO_2 into the oxidizer (Papers IV and V). The aims of the gas-fired experiments were to evaluate different SO_3 measurement techniques (see Section 3.1) and to determine the levels of SO_3 formation under various air-fired and oxy-fuel combustion conditions. During the SO_3 measurement campaign, it became obvious that SO_3 formation increased with increasing temperature in the furnace. The temperature in the furnace was quantified by calculating the average furnace wall temperature from 14 continuously logged thermocouples placed 2 cm from the inner surface of the furnace wall. The typical temperature pattern for the average furnace wall temperature during an operational day is shown in Figure 3.9.

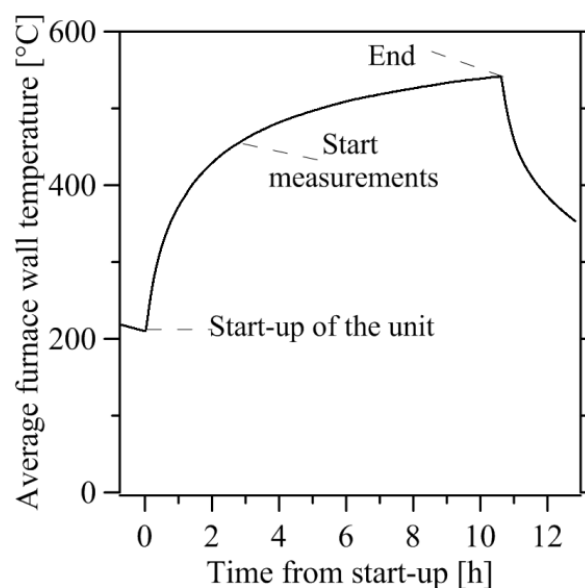


Figure 3.9 Typical average furnace wall temperature pattern during an operational day (Paper V).

Table 3.3 shows the main experimental test conditions during the gas-fired experiments, as well as the flue-gas concentrations of O₂, SO₂, H₂O, and CO₂. The fuel input was equivalent to 60 kW_{th} in all cases, except for the one OF30 case with 75 kW_{th}. The designation OF30 signifies an O₂ concentration of 30 vol.% in the feed gas on a dry basis. The SO₂ concentration in the OF30 case was set at 3000 ppm on a dry basis, which is equivalent to an SO₂ concentration of 2438 ppm on a wet basis. The OF25, OF35, and OF40 cases were adapted to the same SO₂ concentration on a wet basis. The oxygen-to-fuel equivalence ratio, λ , for the OF30 case was set at 1.25. The outlet O₂ concentration was kept constant in all cases, which resulted in different λ values for the different cases. Since it is likely that a wet flue-gas recycle will be applied for industrial oxy-fuel applications, an oxy-fuel case with wet flue-gas recycle was implemented. The feed gas O₂ concentration was 46 vol.% on a dry basis (27 vol.% on a wet basis), hereinafter referred to as OF46w. The concentration of SO₂ and the λ value was varied in additional experiments, which are not listed in Table 3.3.

Table 3.3 Experimental conditions used in the test cases.

Test case	O ₂ in feed gas [vol.%, dry]	Type of FGR	Oxidizer volume flow [m ³ (STP)/h]	λ	Flue-gas composition (M13) (on wet basis)			
					X_{O_2} [%]	X_{SO_2} [ppm]	X_{H_2O} [%]	X_{CO_2} [%]
OF30	30	dry	50.1	1.25	5.39	2438	18.7	~71
OF25	25	dry	63.0	1.31	5.39	2438	15.6	~74
Air	21	-	77.7	1.38	5.39	885	12.0	8.6
OF25 (low SO ₂)	25	dry	63.0	1.31	5.39	885	15.6	~74
OF30 (low SO ₂)	30	dry	50.1	1.25	5.39	813	18.7	~71
OF30 75 kW _{th}	30	dry	62.6	1.25	5.39	1625	18.7	~71
OF46w	46	wet	56.5	1.28	5.39	870 & 1379	54.0	37.9
OF35	35	dry	41.6	1.21	5.39	2438	21.8	66.9
OF40	40	dry	35.6	1.18	5.39	2438	24.7	64.6

The concentration of SO₃ after the furnace (at position M8) was measured using the controlled condensation method for all the cases. The salt method, the isopropanol absorption bottle method, the Pentol SO₃ monitor, and the acid dew-point meter were applied mainly to the OF30 and air-fired cases. The controlled condensation method was used as the standard for comparison, and the SO₄²⁻ concentration in the 5 vol.% isopropanol solution was analyzed by ion chromatography (using the ICS-90 Ion Chromatography System from DIONEX).

In-flame SO₃ concentrations were measured along the center line of the furnace from M2 to M5 for the air-fired, OF30, OF25, and OF25 (low SO₂) cases. Table 3.4 lists the distance from the burner inlet to each furnace measurement level used during the in-flame measurements (M2 to M5). In addition to the SO₃ measurements, the concentrations of SO₂, O₂, and CO, as well as the flame

temperatures were recorded, to characterize the flames (Paper IV). A standard water-cooled suction pyrometer with a type B thermocouple was used to measure the flame temperature. The thermocouple was shielded with a ceramic tube.

Table 3.4 Furnace measurement points.

Measurement position/level	Distance from burner inlet [m]
M2	0.215
M3	0.384
M4	0.553
M5	0.800

Figure 3.10 shows photographs of the flames taken at position M2 for the test cases in Table 3.3. The refractory burner cone is visible at the top of each image. The OF25 flame (b) was completely blue, i.e., free of soot, whereas the air-fired flame (c) showed yellow streaks. The OF30 case (a) and the OF46w case (d) showed relatively blue flames, albeit with some yellow streaks. The OF35 case (e) had a more turbulent and yellow flame than the OF30 case (a), while the flame shape was similar. The OF40 (f) flame was completely yellow with intense soot formation but without a clear flame shape due to the substantial reduction in volumetric gas flow. Intense soot formation is believed to be due to poor mixing conditions in combination with high combustion temperatures. To recall, an increasing OF number means a decreased feed gas volume flow and an increased concentration of O_2 in the feed gas.

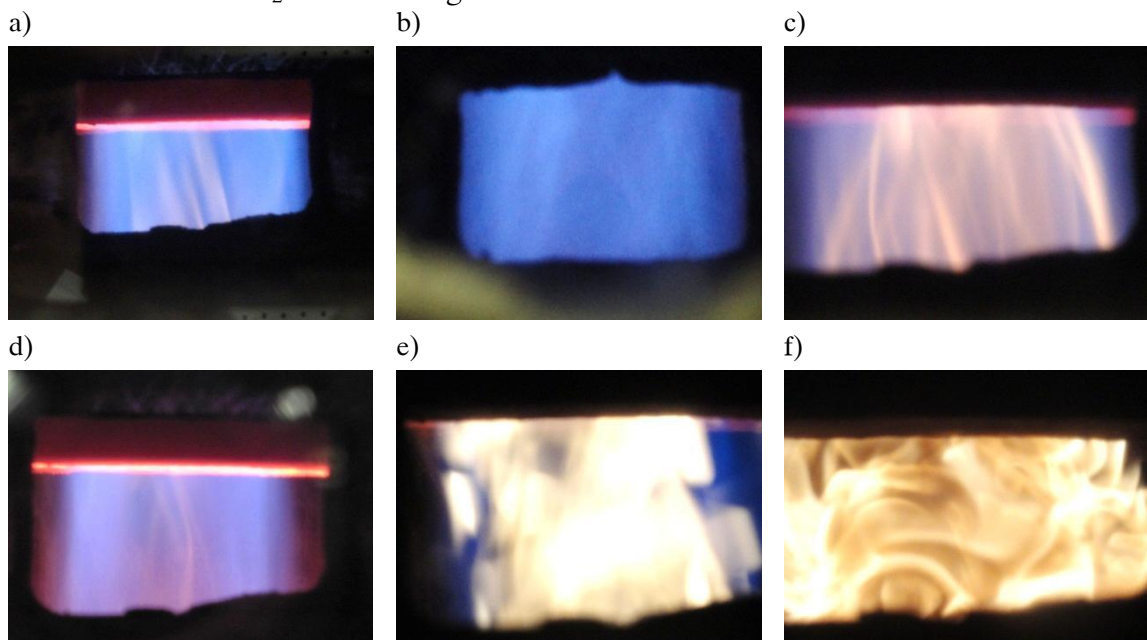


Figure 3.10 Photographs of the flames under the different operating conditions (see Table 3.3): a) OF30; b) OF25; c) air-fired; d) OF46w; e) OF35; and f) OF40. The burner cone is visible at the top of each image.

Figure 3.11 gives the measured temperature profiles along the center line of the furnace for the air-fired, OF30, and OF25 cases. The temperature profiles of the air-fired and OF30 cases were similar, except at the end of or after the flame (M5), where the temperature in the OF30 case was lower than that in the air-fired flame, mainly due to the reduced volumetric flow of the feed gas in the OF30 case. The OF25 conditions resulted in a flame temperature level approximately 100°C lower at the center line from M2 to M4, as compared with the air-fired case.

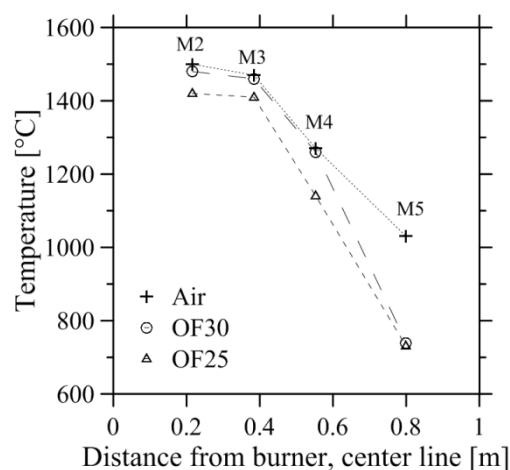


Figure 3.11 Measured temperature profiles along the center line of the furnace for the air-fired, OF30, and OF25 cases (Paper IV).

3.3 Plug-Flow Reactor Experiments

Plug-flow reactor experiments were performed at the Aragón Institute of Engineering Research at the University of Zaragoza, with the aims of investigating SO_3 formation under post-flame conditions and validating a detailed chemistry model.

The experimental setup consisted of a gas feeding system, a reactor system, and a gas analysis system. The reactor system, as shown in Figure 3.12a, consisted of a simple quartz glass tube (reactor) inserted in a one-zone electrically heated oven. The quartz glass reactor had an inner diameter of 45.5 ± 0.5 mm and a length of 900 mm. Different gas mixtures were injected at the top of the reactor. A measurement matrix with all the test cases is presented in Paper VI (Table 1).

Experiments were performed mainly in the temperature range of 800 K to 1473 K. A temperature of 1473 K was recommended as the maximum temperature for the quartz reactor by the manufacturer. Nevertheless, some tests were performed at the higher temperatures of 1573 K and 1673 K. Figure 3.12b shows the axial temperature profile inside the reactor, measured with a type K thermocouple, for different set-points of the oven. The temperature in the reactor reaches almost

the set-point temperature of the oven and an almost isothermal temperature is attained in the reactor throughout a zone of 200 mm. This zone is denoted as the ‘isothermal reaction zone’ and the set-point of the oven is designated as the experimental temperature T_e . Figure 3.13 shows as an example the gas residence time for $T_e = 1473$ K in the isothermal reaction zone and downstream during gas cooling. The gas cooling takes approximately 5 seconds, which is similar to the gas residence times expected for coal-fired boilers (see Senior et al.⁸³).

The SO_3 concentration at the outlet of the reactor was measured with the controlled condensation method. The amount of SO_4^{2-} in the isopropanol solution was analyzed immediately by titration with 0.01 mol/l sodium hydroxide (NaOH).

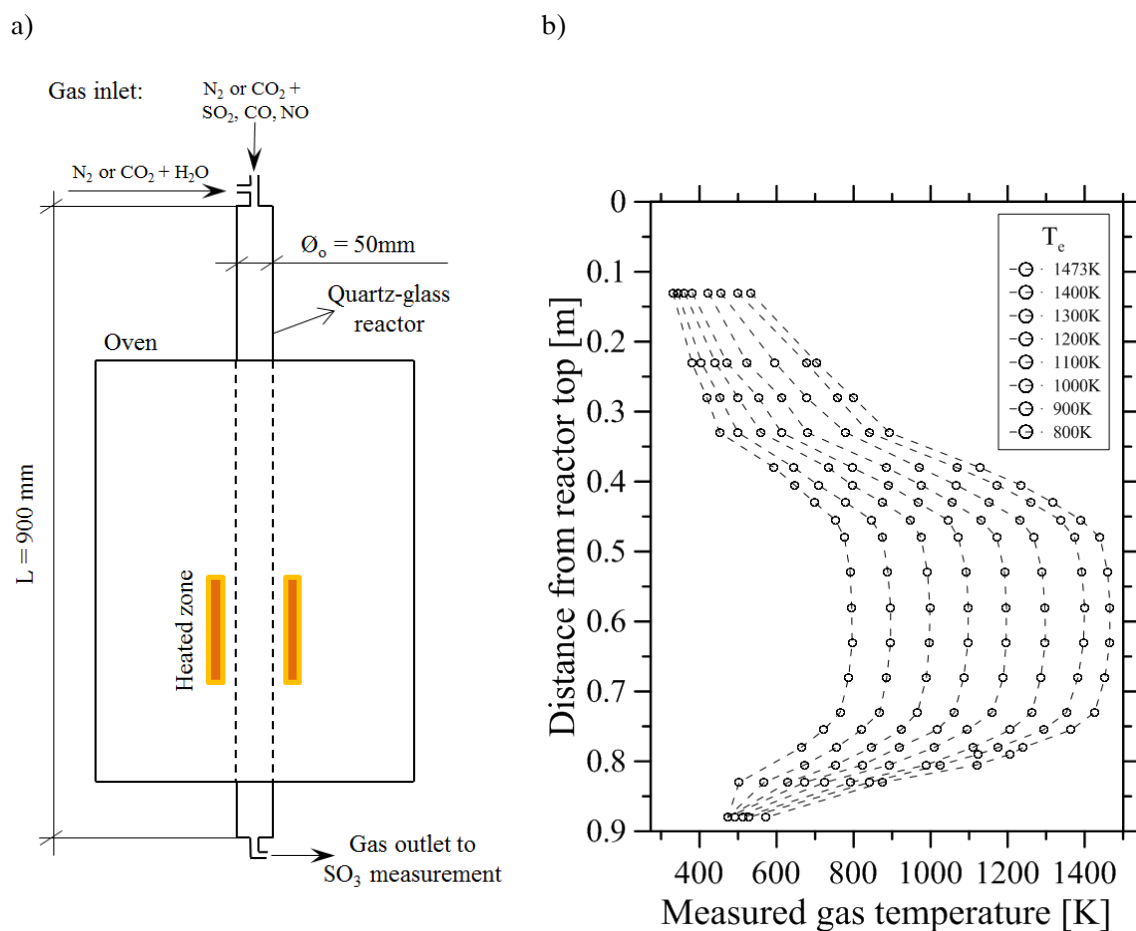


Figure 3.12 Experimental setup: a) Quartz reactor and the one-zone electrically heated oven; and b) Axial temperature profiles measured in the quartz glass reactor for different experimental temperatures, ranging from 800 K to 1473 K (Paper VI).

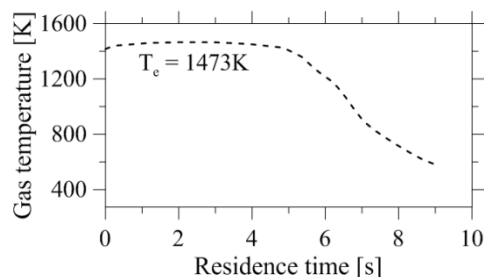


Figure 3.13 Residence times in the isothermal reaction zone and gas cooling for $T_e = 1473$ K.

3.4 Modeling Work

The gas-phase chemistry related to sulfur species was investigated using detailed gas-phase reaction models. The formation of SO_3 was of special interest. The detailed gas-phase mechanism proposed by Giménez-López et al.⁸⁴, which is based on a mechanism reported by Alzueta et al.⁸⁵, was used in the models. Giménez-López et al.⁸⁴ validated the mechanism for the oxidation of carbon monoxide (CO) in the presence of SO_2 in CO_2 and N_2 atmospheres. The formation of H_2SO_4 (Reaction 1) was not included in the mechanism, but it should be kept in mind that at 200°C , almost all the “ SO_3 ” is present in the form of gaseous H_2SO_4 . The reactions and rate constants of the mechanism are listed in the Appendix to this thesis. The calculations were performed with the CHEMKIN-PRO⁸⁶ software and a plug flow was assumed in the models.

In Paper III, general differences with respect to SO_3 concentrations between oxy-fuel and air-fired combustion were investigated using a detailed gas-phase reaction model. The temperature profile of the plug-flow reactor was predefined using an approach similar to that described in Paper I. It should be mentioned here that the mechanism used in Paper I has not been validated for oxy-fuel conditions with respect to sulfur chemistry. The temperature profiles applied in the work in Paper III are presented in Figure 3.14; a linear temperature profile from 1900 K to 400 K and a temperature profile typical of a pulverized coal-fired power plant from Senior et al.⁸³ are depicted.

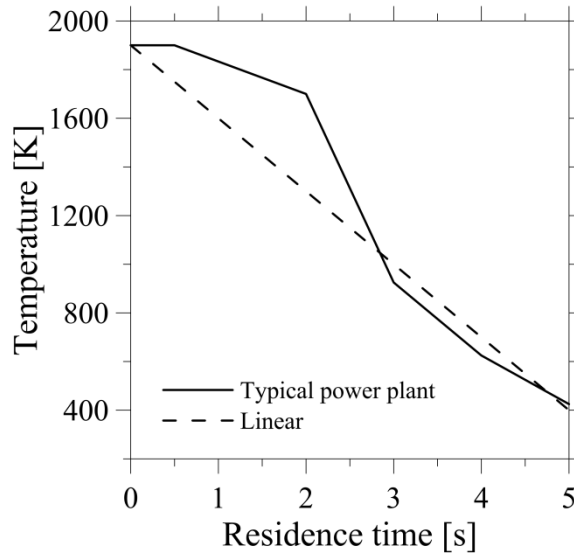


Figure 3.14 Predefined temperature profiles of the plug-flow reactor model described in Paper III. A linear temperature profile (dotted line) and a temperature profile typical of a pulverized coal-fired power plant (solid line, from Senior et al.⁸³) are shown.

Different gas concentrations were used as the input data for the plug-flow reactor in Paper III. The cases are presented in Table 3.5 and include an air-fired case (Air) and five oxy-fuel cases (Oxy1 to Oxy5) with various concentrations of SO₂ and recycling types (wet or dry). The gas concentrations are based on theoretical flue gas compositions from lignite combustion (Table 3.1) under air-fired and oxy-fuel conditions. Oxy1 represents an oxy-fuel case with dry recycling and Oxy2 represents an oxy-fuel case with wet recycling, both without SO₂ in the flue-gas recycle. Oxy3 represents an oxy-fuel case with dry recycling and a conversion rate for fuel sulfur to SO₂ of 45%, as estimated from experiments with the Chalmers oxy-fuel test unit (Paper II). Oxy4 and Oxy5, which are oxy-fuel cases with dry and wet recycling, respectively, assume that all the fuel sulfur is converted to SO₂.

Table 3.5. Gas composition of the test cases used as input data for the calculations presented in Paper III.

	Air	Oxy1	Oxy2	Oxy3	Oxy4	Oxy5
Type of recycling	-	dry	wet	dry	dry	wet
Conversion of coal sulfur to SO ₂	100%	(17%)	(25%)	45%	100%	100%
SO ₂ [ppm]	750	750	750	1968	4363	3014
O ₂ [vol. %]	2.8	2.8	2.8	2.8	2.8	2.8
CO ₂ [vol. %]	15.1	b.d. ^a				
H ₂ O [vol. %]	9.1	9.1	36.4	9.1	9.1	36.4
NO [vol. %]	0.04	0.04	0.04	0.04	0.04	0.04
N ₂ [vol. %]	b.d. ^a	0.4	0.4	0.4	0.4	0.4

^a By difference

Flue-gas composition data from the lignite-fired experiments in the Chalmers oxy-fuel test unit (see Table 3.2) were used as the input data for a plug-flow reactor model to estimate the concentrations of SO₃ in the flue gas. The flue-gas composition data are given in Table 3.6 for the air-fired, OF30, and OF43w cases. The temperature profile presented by Senior et al.⁸³ (see Figure 3.14) was used as the input data, although longer residence times were used. The main objective was to derive general trends rather than accurate predictions, and the applied temperature profile can be considered as an acceptable approach for the Chalmers oxy-fuel unit.

Table 3.6 Conditions and flue-gas composition (on wet basis) used in the calculations based on the test cases performed in the 100-kW_{th} Chalmers oxy-fuel test unit (see Table 3.2).

	Air	OF30	OF43w
Estimated residence time [s]	10	13	14
Conversion of coal sulfur to SO ₂ (C _{SO2})	67%	41%	46%
Flue-gas composition per volume			
SO ₂ [ppm]	500	1660	1290
O ₂ [%]	3.0	4.9	4.9
CO ₂ [%]	15.0	79.3	59.8
H ₂ O (calculated) [%]	9.0	13.2	34.1
NO (assumption) [ppm]	400	400	400
Remainder, assumed as N ₂ [%]	72.9	2.4	1.0

In Paper IV, the concentrations of SO₃ along the center line of the furnace were modeled and compared with the measured concentrations of SO₃. The temperature profiles measured along the center line (Figure 3.11) were used as the input data, and the furnace was considered as a plug-flow reactor. The fuel (C₃H₈) and the recycled flue gas without O₂ were injected at the inlet of the plug-flow reactor and O₂ was injected gradually to match the measured O₂ concentrations along the center line of the furnace. The gradual injection of O₂ should capture the mixing conditions at the center line of the experimental furnace. This approach was validated and successfully applied in previous modeling work of the same experimental unit.⁸⁷

In Paper VI, the experiments performed in the quartz reactor (Figure 3.12a) were modeled with a detailed gas-phase kinetic model for interpretation and discussion of the measured concentrations of SO₃. The measured temperature profiles in Figure 3.12b, as well as the gas concentrations given in Paper VI (Table 1) were used as the input data. Perfect mixing is assumed since the gases are mixed upstream of the reactor.

4 - Results and Discussion

This Chapter provides a summary of the work carried out in this thesis. Key results from the papers are briefly discussed, together with some additional results not included in the papers.

4.1 Gas-Phase Sulfur Chemistry in Air and Oxy-Fuel Atmospheres

4.1.1 Equilibrium Considerations for Gaseous Sulfur Species

Figure 4.1 shows the equilibrium distributions of sulfur species in the gas-phase at 1500 K for the air-fuel conditions (a) and for oxy-fuel conditions with a wet recycle (b). The gas input data were based on the lignite used in the Chalmers oxy-fuel test unit (Table 3.1). The total molar amount of all sulfur species is set at 100% for each stoichiometry. It is clear from Figure 4.1a and b that, under fuel-lean conditions, it is mainly SO_2 and small amounts of SO_3 that remain. There are no differences between the oxy-fuel case and the air-fired case under the fuel-lean conditions, and the SO_3/SO_x ratio is 1% for a stoichiometry of 1.5 for both cases. H_2S , HS_2 , and SO_2 are the dominant species under fuel-rich conditions. However, not all gaseous sulfur species are included in the mechanism (for example, carbonyl sulfide) and the mechanism is not validated for all the conditions presented in Figure 4.1a and b. The difference between the oxy-fuel and the air-fired case is noticeable in the sub-stoichiometric region, and although H_2S is dominant under air-fired conditions, the concentration of SO_2 is always higher than the concentration of H_2S in the oxy-fuel case. At a stoichiometry of around 1, it is difficult to determine the concentrations of the different sulfur species because small changes in the oxygen content have a strong impact on the compositions of the sulfur species. It should be noted that the distribution of sulfur species represents equilibrium data and the residence time also has to be considered, when dealing with real concentrations in a flame.

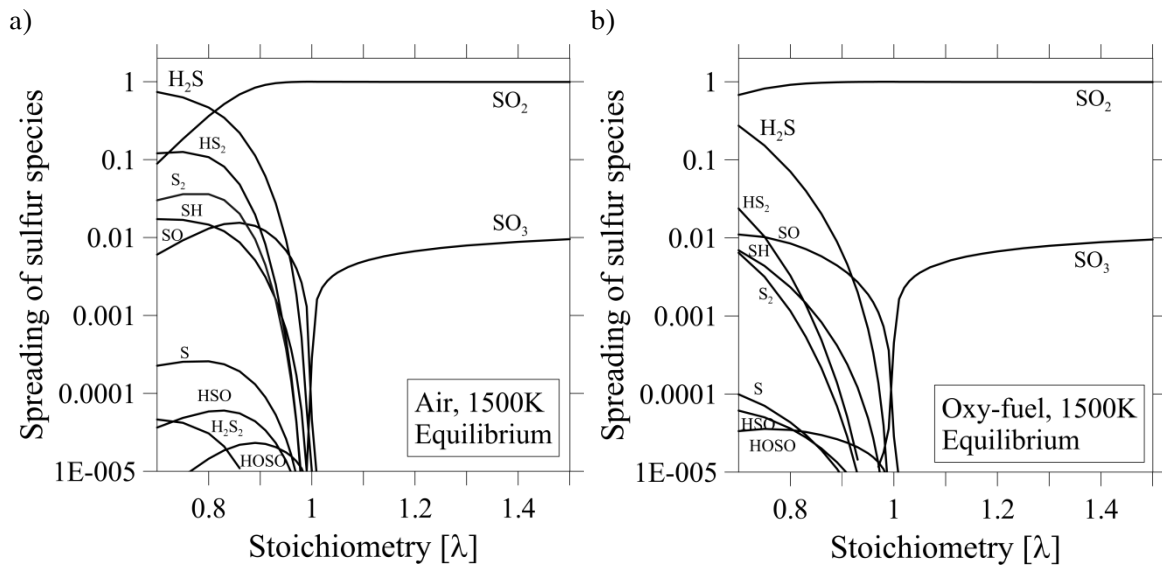


Figure 4.1 Equilibrium distributions of sulfur species in the gas-phase at 1500 K under: a) air-fuel conditions; and b) oxy-fuel conditions with wet recycling. The gas input data of the equilibrium reactor are based on the lignite used in the Chalmers oxy-fuel test unit.

The equilibrium concentrations of SO_2 and SO_3 within a temperature range of 300 K to 1900 K for the gas composition in the Oxy3 case are shown in Figure 4.2a. At high temperatures, almost all of the sulfur is in the form of SO_2 , whereas at low temperatures almost all the sulfur is in the form of SO_3 . Since SO_3 formation slows down with a decrease in temperature, only a minor fraction of SO_2 is normally converted to SO_3 in a combustion process. This is obvious from Figure 4.2b, where the time for reaching 90% of the equilibrium SO_3 concentration is presented. The residence time of the flue gas in a boiler is relatively short, which means that the formation of SO_3 cannot be described by equilibrium calculations, at least not for temperatures lower than around 1400 K.

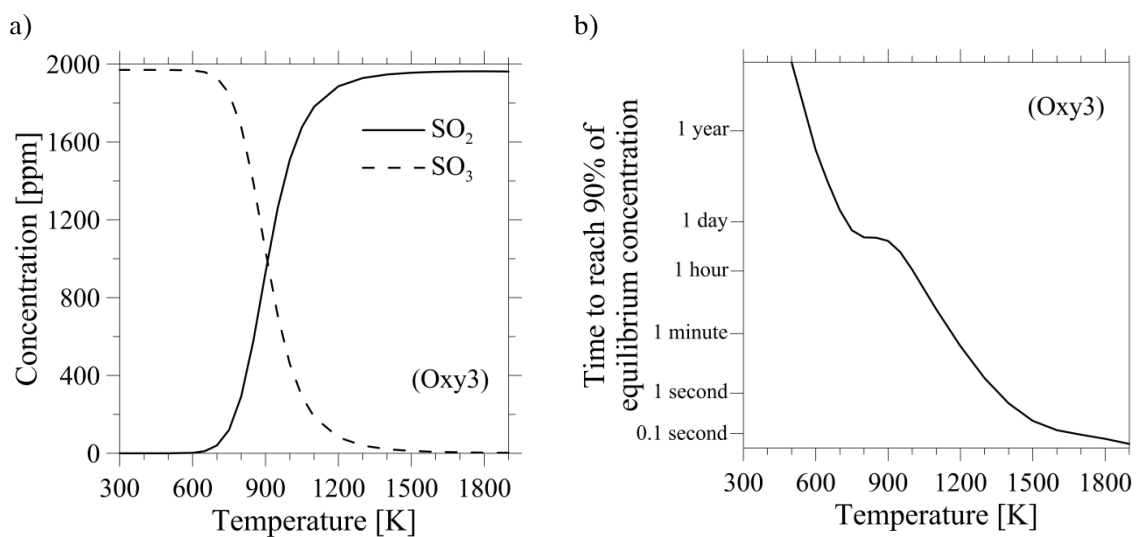


Figure 4.2 a) Equilibrium concentrations for SO_3 and SO_2 with the gas composition in the Oxy3 case within a temperature range of 300 K to 1900 K. b) Time required to reach 90% of the equilibrium concentration of SO_3 as a function of temperature in the Oxy3 case (Paper III).

4.1.2 H₂S Formation

The homogeneous formation of H₂S in the gas phase is modeled in Paper I. Figure 4.3 shows the formation of H₂S during oxy-fuel combustion for different temperatures and stoichiometries ($\lambda = 0.6$ and $\lambda = 0.8$), a reaction time of 1 second, and at equilibrium. The concentration of H₂S is calculated in a flame with an initial SO₂ concentration of 1000 ppm. The formation of H₂S can be considerable under sub-stoichiometric conditions in a flame combined with temperatures of between 1100°C and 1600°C (see also Figure 4.1a and b). The flue gas recycle in oxy-fuel combustion can influence directly the H₂S concentration, as the flame temperature has a considerable impact on H₂S formation under sub-stoichiometric conditions. Furthermore, the type of recycle influences the concentration of SO₂ in the oxidizer. In principle, an increased H₂S concentration is anticipated in an oxy-fuel flame, as compared with an air-fired flame, due to the SO₂ content in the oxidizer. However, future studies should investigate this in detail, as Figure 4.1 shows lower H₂S fractions for the oxy-fuel than for the air-fuel conditions when equilibrium is assumed. In pulverized coal combustion, H₂S is not only formed from SO₂, but also released from organic sulfur compounds²³ in the coal.

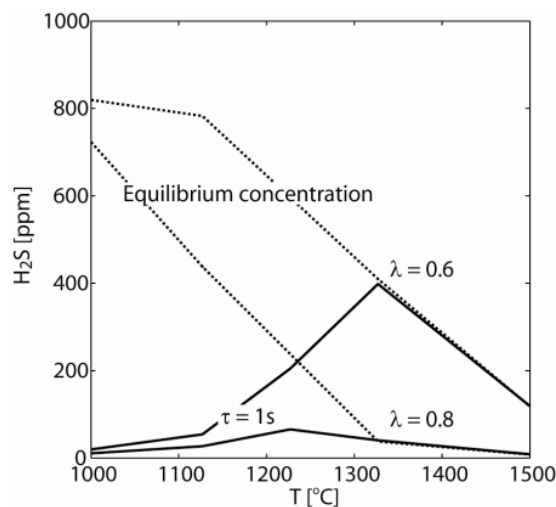


Figure 4.3 H₂S concentrations at equilibrium (dashed line) and after 1 second of reaction time (solid line, τ) at the stoichiometric ratios (λ) of 0.6 and 0.8, and for an initial concentration of SO₂ of 1000 ppm (Paper I).

4.1.3 SO₃ Formation – Experiments and Modeling

This Section presents initially the results obtained from the SO₃ measurements and modeling of the quartz reactor. Thereafter, some modeling results from Paper III are presented. Finally, the measured SO₃ concentrations in the Chalmers oxy-fuel unit are presented and discussed.

Influence of H₂O Concentration on SO₃ Formation

Figure 4.4 shows the measured and modeled outlet concentrations of SO₃ after the quartz reactor for different H₂O concentrations in the absence of combustibles. An increase in water vapor concentration clearly enhances SO₃ formation, as evidenced by the measurements and the model predictions. The agreement between the measured SO₃ concentration and the modeled SO₃ concentration is good, except at 1473 K, where the measurements show significant higher SO₃ concentrations than the modeling results. The model predicts a maximum level of SO₃ formation, which is shifted towards lower temperatures for an increase in H₂O concentration; this phenomenon is not observed in the measurements. The reason for the increase in SO₃ formation caused by elevated H₂O concentration is an increase in the levels of radicals in the reactor. However, if CO is added to the quartz reactor the impact of H₂O concentration on SO₃ formation can be reversed, as discussed in Paper VI.

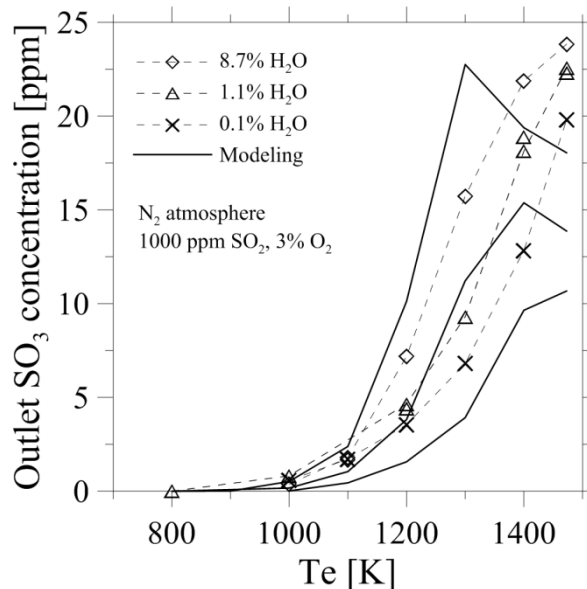


Figure 4.4 Measured (symbols) and modeled (solid lines) concentrations of SO₃ for different H₂O concentrations in the quartz reactor. The inlet gas contains 1000 ppm SO₂ and 3% O₂ on a wet basis in an N₂ atmosphere (Paper VI).

Influence of O₂ Concentration on SO₃ Formation

Figure 4.5 shows the measured SO₃/SO_x conversion ratio of the quartz reactor for different O₂ concentrations and an SO₂ concentration of 1000 ppm. It is clear that the formation of SO₃ is favored by increases in the concentration of O₂, as well as increases in the experimental temperature. The concentrations of O- and OH-radicals increase with increasing O₂ concentration, which promotes SO₃ formation through Reactions 8, 10, and 11. The level of SO₃ formation is low for T_e ≤ 1000 K in all cases. For example, at an O₂ concentration of 3%, less than 1 ppm SO₃ was detected at T_e = 1000 K, and no SO₃ was detected at T_e = 800 K. This is in accordance with the results of Flint and Lindsay⁸⁸.

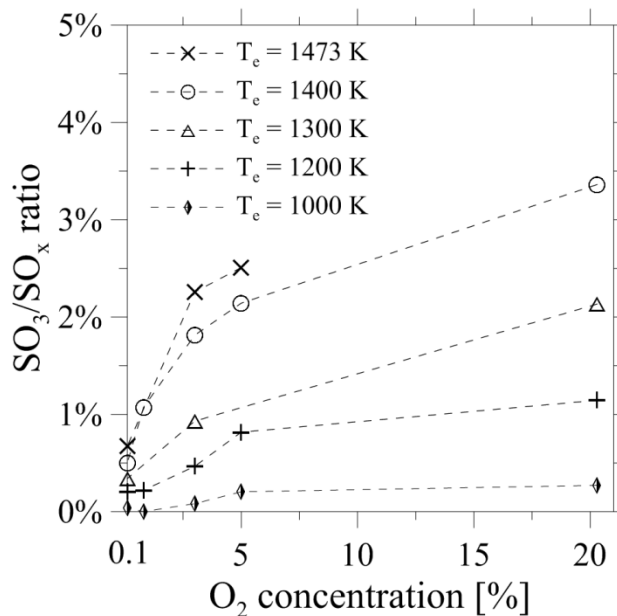
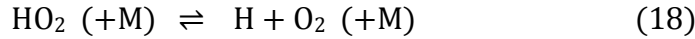


Figure 4.5 Measured SO₃/SO_x ratios (symbols) for different O₂ concentrations (0.1%, 0.8%, 3.0%, 5.0%, and 20.3%) in the quartz reactor (1000 ppm SO₂; N₂ atmosphere; without combustibles).

SO₃ Formation in N₂ and CO₂ Atmospheres

Figure 4.6a compares the measured and modeled outlet concentrations of SO₃ after the quartz reactor in a CO₂ atmosphere and in an N₂ atmosphere in the absence of combustibles, and Figure 4.6b shows the results when 1000 ppm CO was added at the inlet of the quartz reactor. In the absence of combustibles (Figure 4.6a), the measured, as well as the modeled, SO₃ concentrations show an increase in SO₃ formation in the CO₂ atmosphere, as compared with the N₂ atmosphere for all the experimental temperatures. The difference is most pronounced at T_e = 1300 K, where the measured SO₃ concentration is 30% higher

and the modeled SO_3 concentration is 44% higher in the CO_2 atmosphere. The formation of SO_3 is more sensitive to the reactions:



in a CO_2 atmosphere than in an N_2 atmosphere. The formation of H-radicals is increased by Reaction 18 due to the decomposition of hydroperoxyl radicals (HO_2), which are mainly formed from Reaction 11. This increases the formation of O- and OH-radicals in Reaction 14, and thereby increases SO_3 formation. Furthermore, the 3rd body efficiency in Reactions 8 and 10 for CO_2 is higher than for N_2 .⁸⁴ The effect of CO_2 on the O/H radical pool has been discussed by Glarborg and Bentzen⁶³ and by Abián et al.⁸⁹.

For the experiments with 1000 ppm CO in the inlet gas (Figure 4.6b), a decrease in SO_3 formation was noted in the CO_2 atmosphere, as compared to the level in the N_2 atmosphere. The model predictions show the same tendency as the experimental results, except for $T_e = 1400 \text{ K}$ and $T_e = 1473 \text{ K}$. The measured SO_3 concentration is in good agreement with the model predictions for $T_e = 1100 \text{ K}$, and shows a reduction of around 80% in SO_3 concentration for the CO_2 atmosphere. During the combustion of CO, Reaction 18 is reversed (HO_2 production) in both atmospheres due to the elevated concentrations of H, although the rate is higher in the CO_2 atmosphere. SO_3 is then consumed during CO combustion by the reverse of Reaction 11, which is more pronounced in the CO_2 atmosphere.

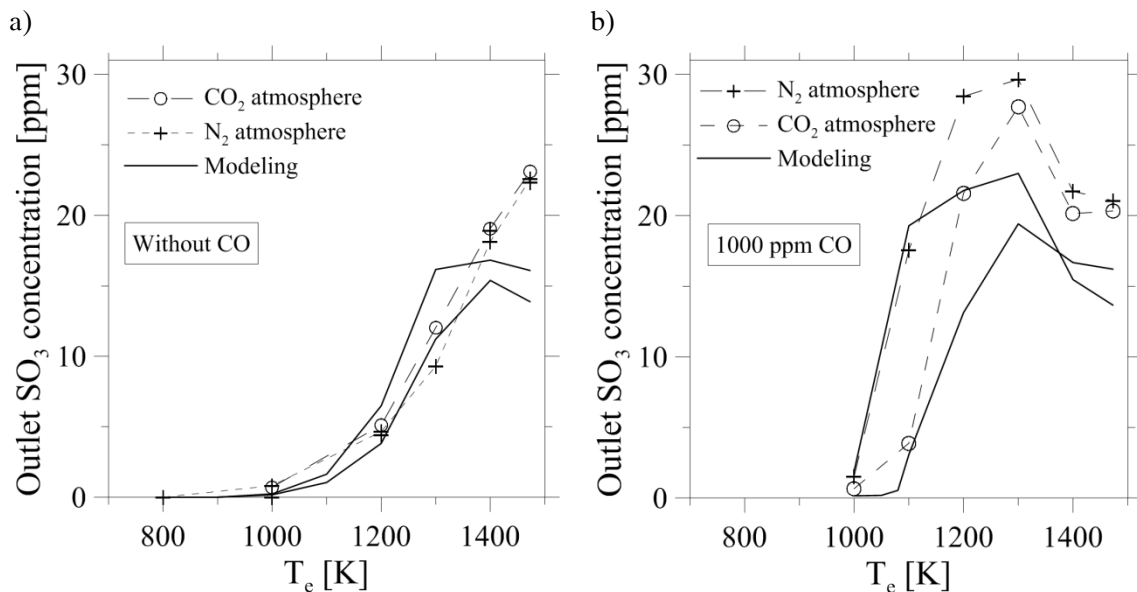


Figure 4.6 Comparison of SO_3 formation levels in CO_2 and N_2 atmospheres. Measured SO_3 concentrations are shown as symbols, and model predictions are shown as solid lines. The inlet gas contains 1000 ppm SO_2 , 3% O_2 , and either (a) 0 ppm CO or (b) 1000 ppm CO (Paper VI).

Impact of the Burnout Region on SO₃ Formation

Figure 4.7a shows the calculated SO₃ concentrations in the flue gas versus O₂ concentrations at a fixed temperature of 1173 K for the Oxy3 case (~2000 ppm SO₂). The calculation was performed for residence times of 0.5, 1.0, and 2.0 seconds. These conditions may be relevant, for example, to the superheater region of a power plant. The concentration of SO₃ increases for increases in O₂ concentration and residence time. The results shown in Figure 4.7b were calculated using the same conditions as in Figure 4.7a, albeit with a CO concentration of 2000 ppm. This was done because there may be zones in a boiler that correspond to such conditions, e.g., the burnout zone. Comparing the data in Figure 4.7a and b, it is evident that the presence of CO significantly increases SO₃ formation, as discussed above. Since the oxidation of CO is relatively fast and the amount of CO limited, the influence of CO on SO₃ formation is more pronounced for short residence times. To summarize, the boiler zone that has moderate temperatures (~1200 K, i.e., conditions typical of the convective pass) and where there is an excess of oxygen is critical with respect to the formation of SO₃, especially when CO is available.

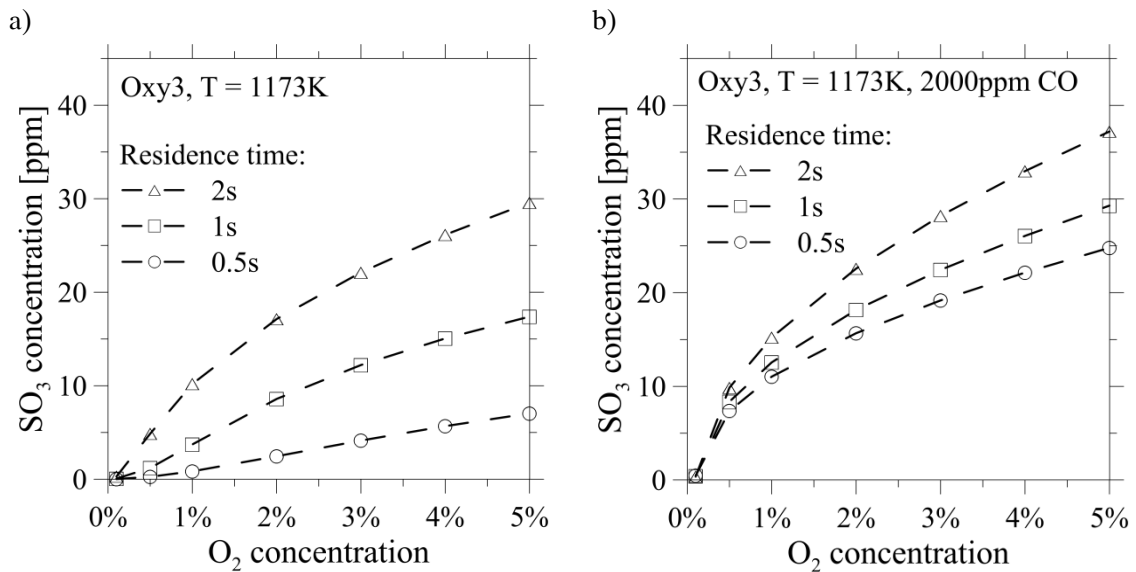


Figure 4.7 Influences of O₂ concentration and residence time on SO₃ formation at 1173 K with 1968 ppm SO₂ in the inlet of the plug-flow reactor without CO (a), and with 2000 ppm CO in the inlet of the plug-flow reactor (b) (Paper III).

Experiments with the Chalmers Oxy-Fuel Unit: Impact of λ on SO_3 Formation

Figure 4.8 shows the influence of the oxygen-to-fuel equivalence ratio, λ , on the SO_3/SO_x ratio for the OF30 and air-fired cases. The SO_3/SO_x ratio increases with increasing value of λ . However, the impact of λ on the SO_3/SO_x ratio in the data shown in Figure 4.8 is not as significant as it would be in a simple plug-flow model. This is partly due to mixing effects since, a wide range of oxygen-to-fuel ratios will be represented in the flames regardless of the global λ . In addition, both the residence time and the flame temperature increase when the λ in the test unit is decreased. With respect to industrial applications, it should be mentioned that when λ is reduced, the concentration of SO_2 increases, assuming that the burnout of sulfur from the fuel is not affected, as this would counteract the benefit of reduced SO_3 formation at reduced λ values.

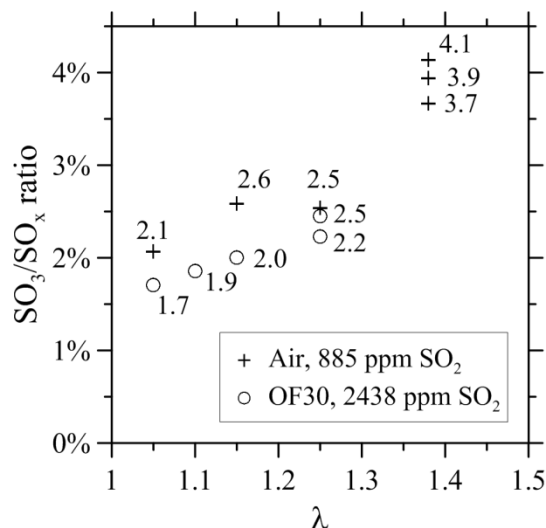


Figure 4.8 SO_3/SO_x ratios for different λ values for the OF30 case with an SO_2 concentration of 2438 ppm and for the air-fired case with an SO_2 concentration of 885 ppm.

SO_3 Formation during Air-Fired and Oxy-Fuel Combustion

Figure 4.9 shows the measured concentrations of SO_3 for the air-fired case and for the OF25 and OF30 cases with low concentrations of SO_2 . The amount of SO_3 formed in the OF25 case was less than half of that formed in the air-fired case. The OF30 case yielded a somewhat lower outlet concentration of SO_3 than the air-fired case. The flame temperature and the average furnace wall temperature in the OF25 case were significantly lower in the OF25 case than in the air-fired case (see Figure 3.11 and Figure 4.9). This probably accounts for the lower concentration of SO_3 in the OF25 case compared with the other cases. Crumley and Fletcher⁹⁰ detected an increase in SO_3 formation for an increase in the temperature of the furnace, and they concluded that this was most probably due

to an increase in the concentration of O-radicals. The higher SO₃ concentration in the air-fired case compared to the OF30 case can be explained by the significantly higher temperature at measurement point M5 (see Figure 3.11) combined with a relatively high concentration of O₂ at M5, as discussed in Paper IV. The CO₂ atmosphere may also have influenced SO₃ formation in the oxy-fuel cases, as discussed above (Figure 4.6), although it is expected that the temperature in the furnace is the main reason for the increased concentrations of SO₃ in the air-fired case.

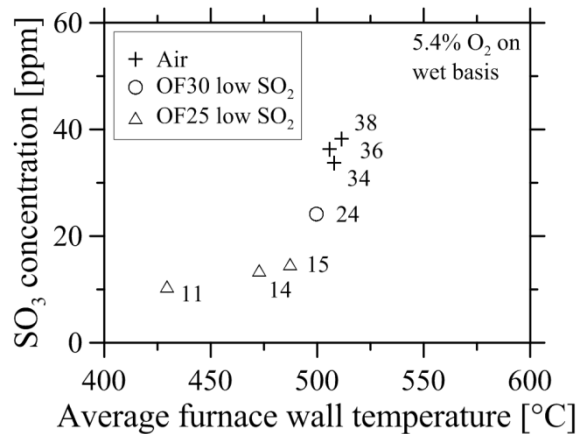


Figure 4.9 Measured outlet concentrations of SO₃ in the air-fired, OF25, and OF30 cases with low concentrations of SO₂ (see Table 3.3) (Paper IV).

Influence of FGR Conditions on SO₃ Formation

Figure 4.10 shows the measured acid dew-point temperatures for four oxy-fuel cases with different flue gas recycle (FGR) ratios in the Chalmers oxy-fuel unit. It is clear that the acid dew-point temperature increases for a decrease in FGR ratio. This behavior could be validated by SO₃ measurements. Figure 4.11 shows the measured SO₃/SO_x ratios for the OF25, OF30, and OF40 cases. SO₃ formation was significantly enhanced in the OF30 case, as compared with the OF25 case. The measured SO₃/SO_x ratio was highest in the OF40 case. In general, the increase in SO₃/SO_x ratio with increasing OF number, i.e., reduced FGR ratio, can be explained by an increase in both the H₂O concentration and the average temperature in the furnace, due to an increase in flame temperature caused by reduced gas volume. Furthermore, the residence time is prolonged with a decrease in FGR ratio, which also leads to a higher concentration of SO₃ in the flue gas. The increased concentration of O₂ in the feed gas might also contribute to increased SO₃ formation. However, the concentration of O₂ after combustion was the same in all cases.

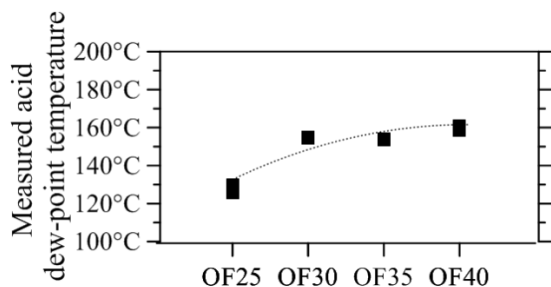


Figure 4.10 Measured acid dew-point temperatures for the OF25, OF30, OF35, and OF40 cases.

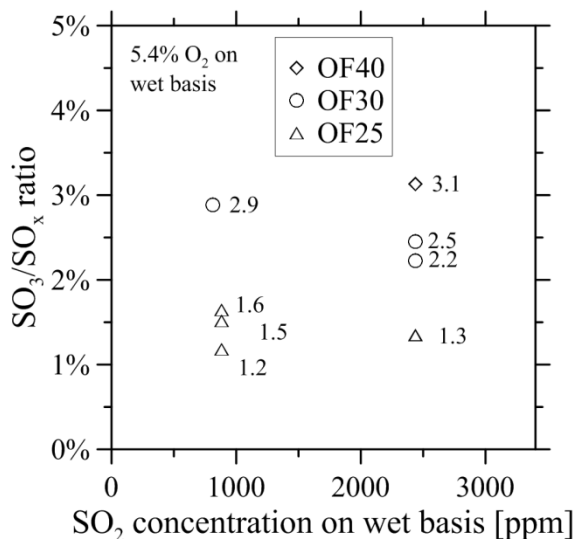


Figure 4.11 Influence of FGR ratio on the SO₃/SO_x ratio.

Figure 4.12 compares the measured outlet concentrations of SO₃ for an oxy-fuel case with a dry recycle (OF30) and an oxy-fuel case with a wet recycle (OF46w) for different concentrations of SO₂ in the flue gas of the Chalmers oxy-fuel unit. The measurements show an increase in outlet SO₃ concentration for oxy-fuel combustion with the wet recycle. For an industrial oxy-fuel plant, the SO₂ concentration will be lower for wet FGR conditions than for dry recycling, as SO₂ enrichment is lower in wet FGR than in dry FGR. This will, to some extent, counteract the effect of enhanced SO₃ formation in the presence of a large concentration of H₂O in the flue gas.

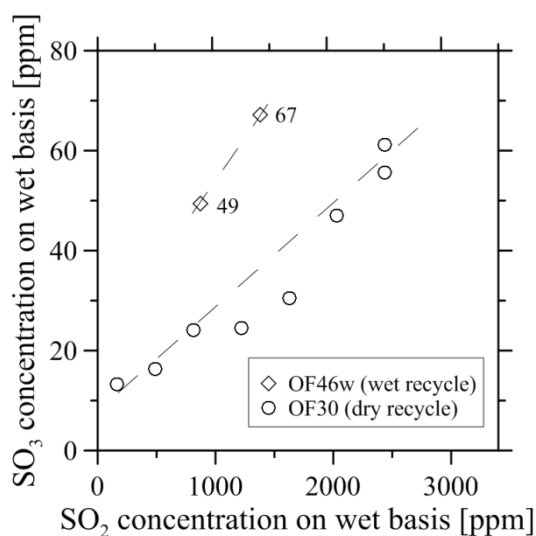


Figure 4.12 Influence of wet FGR on outlet concentrations of SO₃.

4.1.4 Evaluation of the SO₃ Measurement Techniques

Figure 4.13 shows the measured SO₃ concentrations at the furnace outlet in relation to the average furnace wall temperatures for the air-fired case (a) and the OF30 case (b), as obtained using the controlled condensation method, salt method, isopropanol absorption bottle method, and the Pentol SO₃ monitor. It is evident that SO₃ formation increases with increasing temperature in the furnace. Therefore, the furnace temperature has to be taken into account when comparing the results of the measurements.

Surprisingly good results were obtained with all the methods. The largest variations were observed in the data obtained with the isopropanol absorption bottle method. The controlled condensation method and salt method gave comparable results, and the reproducibility of these methods was good.

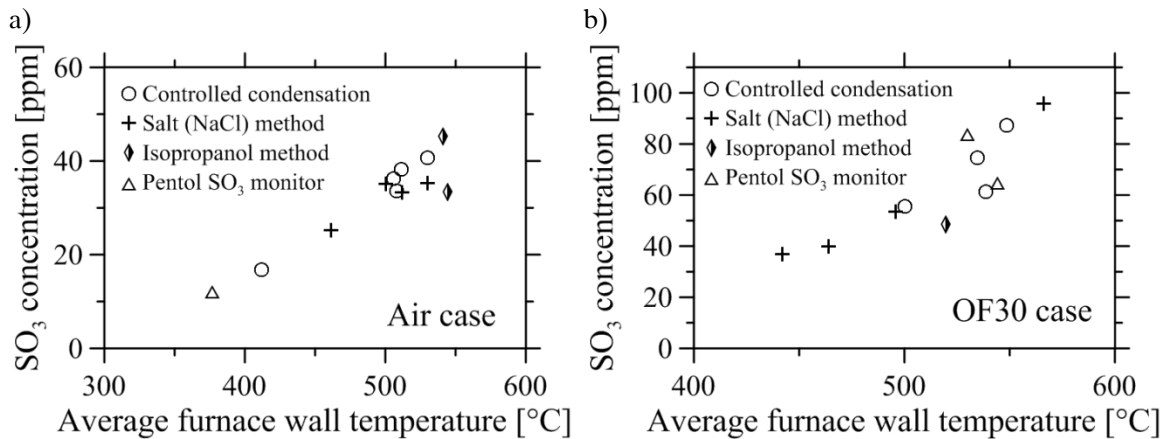


Figure 4.13 Measured SO₃ concentration versus average furnace wall temperature for: (a) the air-fired case; and (b) the OF30 case (Paper V).

Salt Method

Figure 4.14 shows the measured concentrations of SO₃ in the air-fired case versus the time from start-up of the measurements for the salt method. The SO₃ measurement values obtained during controlled condensation are also shown for comparison purposes. The values obtained for SO₃ when using the salt method are quite similar to the measured values obtained from the controlled condensation method. If one considers that the measurements with the controlled condensation method were performed on different days than the measurements with the salt method, the level of agreement between the two measurement methods is good. Similar good results were obtained for measurements performed under oxy-fuel operation (see Paper V). The salt method is currently being evaluated under laboratory conditions by Emil Vainio at Åbo Akademi.

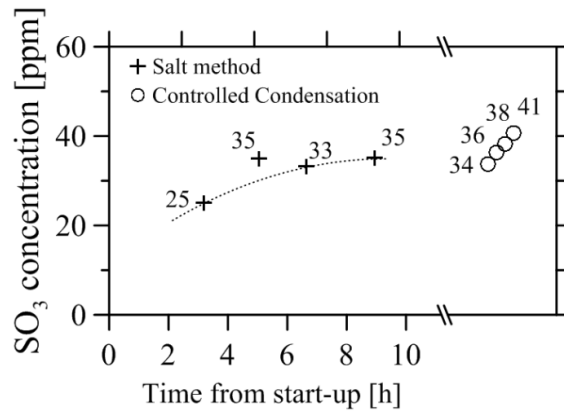


Figure 4.14 Measured concentrations of SO₃ in the air-fired case by applying the salt method.

Isopropanol Absorption Bottle Method

Table 4.1 shows the measured concentrations of SO₃ and SO₂ obtained with the isopropanol absorption bottle method in the air-fired case and OF30 case. A large amount of SO₂ was dissolved in the isopropanol solution, and the obtained SO₂ concentration in the H₂O₂ solution was therefore too low. The amount of SO₂ captured in the isopropanol solution could be reduced by bubbling argon through the isopropanol solution after gas sampling.

The concentrations of SO₃ obtained with the isopropanol absorption bottle method were roughly similar to those obtained with the controlled condensation method, since the sulfate analysis was performed immediately after gas sampling. If the SO₂ dissolved by the isopropanol solution had time to oxidize to sulfate, for example during transportation to a laboratory, a significant error in SO₃ concentration would be expected. However, the differences between the SO₃ concentrations measured using the isopropanol absorption bottle method and those obtained using the controlled condensation method are more significant than the differences in the results between the salt method and the controlled condensation method (see Figure 4.13). Therefore, the isopropanol absorption bottle method is not recommended for SO₃ measurements.

Table 4.1 Concentrations of SO₃ and SO₂ measured with the isopropanol absorption bottle method and the calculated SO₂ concentrations dissolved in the isopropanol.

Case	Average temp. of furnace wall	SO ₃ [ppm]	Sampling time	Purging with argon (1.5 L/min)	SO ₂ measured (in H ₂ O ₂ solution) [ppm]	SO ₂ dissolved in isopropanol [ppm]
Air	541°C	45	30 min	-	350	540
Air	544°C	34	20 min	10 min	570	320
OF30	520°C	49	20 min	15 min	2160	280

Pentol SO₃ Monitor

The Pentol SO₃ monitor was checked in an atmosphere that consisted of moist air and 1000 ppm SO₂. A concentration of SO₃ of almost 10 ppm was displayed by the SO₃ monitor, whereas <1 ppm of SO₃ was detected with the controlled condensation method. For the given minimum purity of 99.8% for the SO₂ from the gas cylinder, the measured SO₃ concentration should be <2 ppm. This test shows that there can be interference by SO₂ when the SO₃ monitor is used.

During the measurements of SO₃ in the OF30 case, the level of agreement between the SO₃ concentrations obtained using the Pentol SO₃ monitor and those obtained using the controlled condensation method was acceptable (see Table 4.2). However, with the controlled condensation method, an increase in SO₃ concentration was obtained for an increase in average temperature of the furnace wall, whereas with the SO₃ monitor a lower SO₃ concentration was measured for an increase in the average temperature of the furnace wall (see Table 4.2). In general, the SO₃ monitor displayed a hysteresis behavior, i.e., the measured SO₃ concentration depended on the previously recorded SO₃ concentration data, with a direct influence on the measurement result. Therefore, the Pentol SO₃ monitor is only recommended if continuous SO₃ measurement or monitoring is of interest.

Table 4.2 Comparison of the Pentol SO₃ monitor and controlled condensation method.

Case	SO ₃ concentration and average temperature of furnace wall		Difference
	Pentol SO ₃ monitor	Controlled condensation method	
OF30, 1500 ppm SO ₂	38 ppm (528°C)	43 ppm (509°C)	-13%
OF30	84 ppm (530°C)	75 ppm (535°C)	12%
OF30	65 ppm (544°C)	87 ppm (548°C)	-26%

Acid Dew-Point Temperature Monitor

It was in principle possible to obtain reasonable acid dew-point temperatures in the flue gases from the air-firing and oxy-fuel combustion using the acid dew-point monitor. However, when the measured acid dew-point temperatures were converted into SO₃ concentrations, major differences with the results from all the other methods applied in the SO₃ measurement campaign were noted. One reason for this is that the concentration of SO₃ is sensitive to the acid dew-point temperature. For example, an acid dew-point temperature of 153°C corresponds to a 50% higher SO₃ concentration than an acid dew-point temperature of 149°C in the air-fired case. Another reason is that the conversion of acid dew-point temperature into SO₃ concentration is uncertain. For an acid dew-point temperature of 144°C in the air-fired case, the correlation of Verhoff and Banchemo¹⁷ gives 16 ppm SO₃ and the correlation of Bolsaitis and Elliott⁹¹ gives

45 ppm SO₃. This means also that the prediction of the acid dew-point from the SO₃ concentration is dependent upon the method used. As a result, for the acid dew-point temperatures measured in the present study, it can be observed with respect to some cases that the correlation of Verhoff and Branchero¹⁷ results in estimated SO₃ concentrations that are too low, whereas the correlation of Bolsaitis and Elliott⁹¹ results in estimated SO₃ concentrations that are too high. Furthermore, in the present study, the acid dew-point monitor seemed to give more accurate readings at flue-gas temperatures close to the acid dew-point temperature than at higher flue-gas temperatures (~400°C).

4.2 Release and Conversion of Sulfur during Coal Combustion

4.2.1 Sulfur Release

The standard method (SS 187177) for analyzing total sulfur in coal assumes that all the sulfur present in the coal is released as SO₂ at 1400°C. An accordant analyzer is the LECO SC 144, which uses sample masses of 1 g and pure O₂ as the combustion atmosphere. This analyzer was applied to investigate the levels of sulfur release at different temperatures from the lignite used in the Chalmers oxy-fuel unit. The results in relation to total lignite mass are illustrated in Figure 4.15, in which the release of coal sulfur as SO₂ at different temperatures is shown. The results match those of a previous investigation by Kasbohm⁹², which included more than 40 lignites (brown coals). The release of sulfur is closely related to temperature. For example, at 1000°C, the amount of sulfur release is around two thirds of the amount released at 1400°C. At temperatures <600°C, the main sources of sulfur release are organically bound sulfur and FeS₂. Thus, the combustion temperature is critical for sulfur release. While these data refer to a system that is in equilibrium, during a combustion process, the residence time is also of importance.

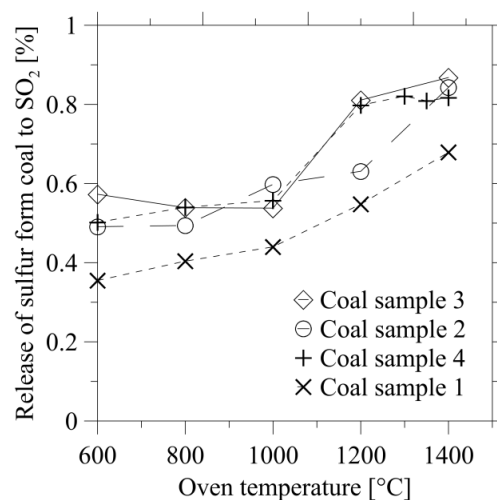


Figure 4.15 Release of sulfur from coal at different temperatures (symbols).

A similar investigation to that conducted for the release of coal sulfur as SO₂ was performed for different ashes. Figure 4.16 illustrates the amounts of sulfur released in relation to the total ash mass at different temperatures. Three ash samples taken from the OF30 case were investigated: a bottom ash sample; a cyclone ash sample; and a fabric filter ash sample. The release of sulfur from the ashes was closely related to the temperature. There was a significant difference between the filter ash and the other samples, in that most of the sulfur from the filter ash was released at 1000°C, whereas the bottom and cyclone ashes exhibited almost no release of sulfur at that temperature. This indicates that sulfur is differentially bound in the various ashes.

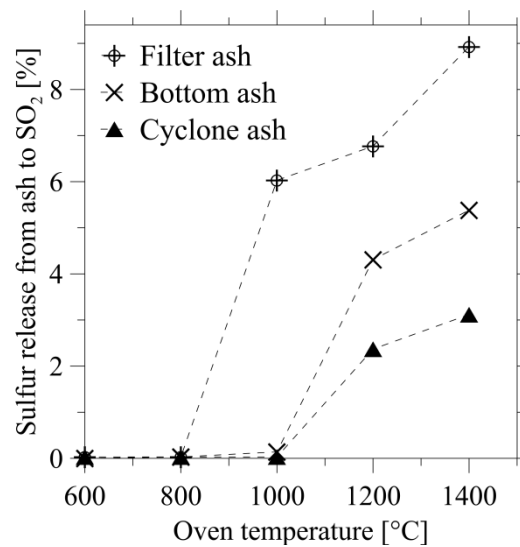


Figure 4.16 Release of sulfur from filter, cyclone, and bottom ashes at different temperatures (symbols). The samples are from the OF30 case. The dashed lines are only included to clarify the data.

4.2.2 The Fate of Sulfur in Oxy-Coal Combustion

Figure 4.17 shows the rate of conversion of coal sulfur to SO_2 (C_{SO_2}), as determined using Equation α above (page 24), for oxy-fuel and air-fired combustion data found in the literature. It is clear from the Figure that the conversion of coal sulfur to SO_2 is lower in oxy-fuel combustion than in air-fired combustion.

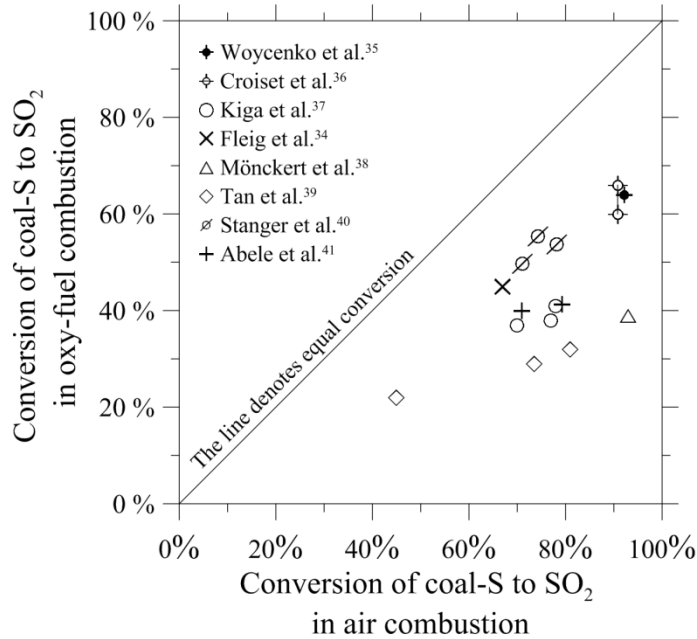


Figure 4.17 Conversion of coal sulfur (coal-S) to SO_2 in oxy-fuel and air-fired combustion in different test units (Paper III).

The fate of sulfur in oxy-coal combustion was investigated by establishing a sulfur mass balance in the Chalmers oxy-fuel unit. The observed concentrations of SO_2 on a wet basis and the conversion rates of coal sulfur to SO_2 (C_{SO_2}) for the air-fired, OF30, OF35, and OF43w cases are presented in Figure 4.18. The concentration of SO_2 was significantly higher in the oxy-fuel cases than in the air-fired case. The concentration of SO_2 on a wet basis was higher in the oxy-fuel cases with dry recycling than in the case with wet recycling due to the lower dilution by water vapor in the flue-gas. The conversion of fuel sulfur to SO_2 was approximately 67% in the air-fired case, 43% in the OF35 case, 41% in the OF30 case, and 46% in the OF43w case. Figure 4.19 shows the corresponding SO_2 emissions (in mg/MJ fuel input) for the different cases. In the oxy-fuel cases, the SO_2 emissions were about 35% lower than in the air-fired case.

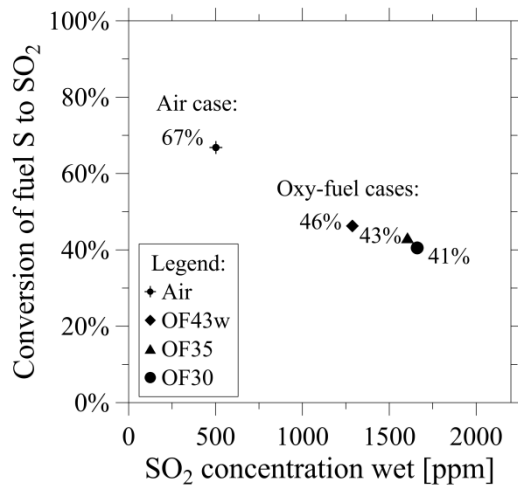


Figure 4.18 Conversion of coal sulfur to SO₂ versus the concentration of SO₂ in the flue gas on a wet basis (Paper II).

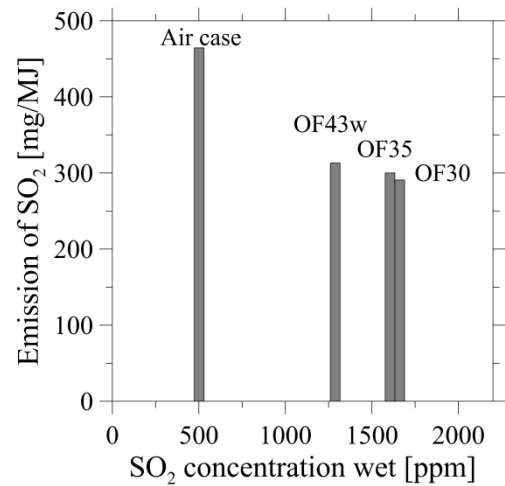


Figure 4.19 Emissions of SO₂ in mg per MJ fuel input versus SO₂ concentration in the flue gas on a wet basis.

The formation of SO₃ was modeled for the coal-fired cases, so as to estimate the concentrations of SO₃ in the flue gas. Figure 4.20 shows the rates of SO₃ formation for the air-fired, OF30 (dry recycle), and OF43w (wet recycle) cases. The flue-gas composition data are given in Table 3.6. The modeled outlet concentration of SO₃ was five-fold higher in the oxy-fuel cases than in the air-fired case due to the higher concentration of SO₂ and excess O₂, as well as the longer residence time. The wet oxy-fuel case (OF43w) had a slightly higher outlet concentration of SO₃ than the dry oxy-fuel case (OF30), although the SO₂ concentration was higher in the OF30 case. This is mainly due to the increased concentration of H₂O in the OF43w case, which favors the formation of SO₃.

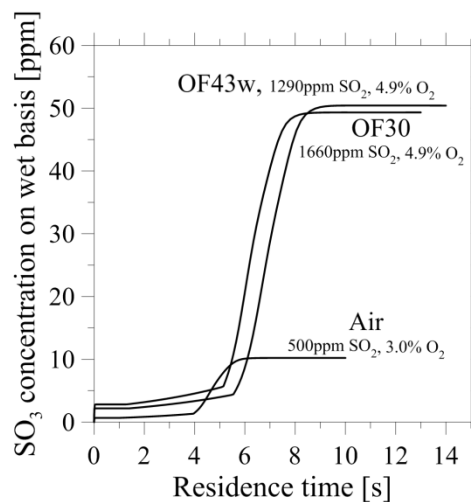


Figure 4.20 Modeled SO₃ formation for the air-fired, OF30, and OF43w cases with a temperature profile typical of a pulverized coal-fired power plant⁸³ (see Figure 3.14).

The lower emissions of SO₂ observed for the oxy-fuel cases can be explained to a limited extent by the higher SO₃ concentrations. Instead, the lower SO₂ emissions implicate a higher concentration of sulfur in the ash or in the condensate from the flue gas condenser. It should be mentioned here that the major proportion of SO₃ in the flue gas will end up in the Ca-rich ash and in the condensate from the flue gas condenser, both of which were analyzed with respect to sulfur content in the present study.

Figure 4.21 shows the theoretical correlation between the sulfur content of the ash and the concentration of SO₂ in the flue gas (4 vol.% O₂) for oxy-fuel combustion with dry recycling, assuming that the sulfur is found in either the stack gas or in the ash (deposits included) after combustion of the lignite (Table 3.1). For example, with a concentration of SO₂ of close to 2000 ppm in the flue gas, the sulfur content of the ash should be around 9% with respect to ash mass, which is equivalent to a sulfur self-retention by ash of around 60%. However, since the mass fraction of sulfur in the ash differed between locations in the Chalmers oxy-fuel unit, the different ash mass flows had to be quantified to establish a sulfur mass balance.

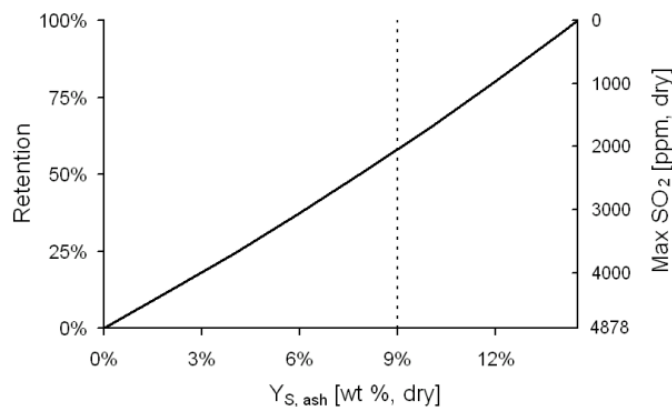


Figure 4.21 Sulfur retention in the ash and remaining concentration of SO₂ in the flue gas during oxy-fuel combustion of lignite (Table 3.1). The dashed line shows an example (Paper I).

Figure 4.22 shows the measured mass flows of the bottom, cyclone, and residual ashes for the air-fired, OF35, and OF43w cases. The mass flow of the cyclone ash was slightly lower and the mass flow of the bottom ash was slightly higher in the oxy-fuel cases than in the air-fired case. The reason for this is that the lower gas volume flow in the oxy-fuel cases decreases the efficiency of the cyclone. Therefore, the mass flow of residual ash was also higher in the oxy-fuel cases than in the air-fired case.

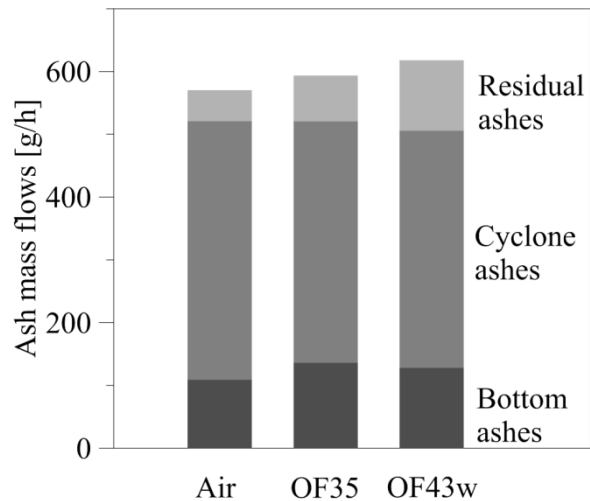


Figure 4.22 Ash mass flows. The residual ash includes all ashes not found as either bottom ash or cyclone ash (Paper II).

Table 4.3 shows the measured sulfur mass fractions in the ashes taken from the bottom of the furnace, the cyclone, the flue-gas cooler, and the fabric filter. From the flue-gas cooler, one sample was taken in the air-fired case and two samples were taken in the OF35 and OF43w cases. All the ashes (including deposits) that were not collected as bottom or cyclone ashes were designated as residual ash. A range for the sulfur mass fraction was defined for the residual ash based on the different sulfur fractions measured in the cooler and filter ashes, which constituted the main part of the residual ash.

Table 4.3 Mass fraction of sulfur in the different ashes. The S fraction of the residual ash is represented by $Y_{S, cooler ash}$ and $Y_{S, filter ash}$.

Test case	Measured mass fraction of sulfur in the ash [%]			
	$Y_{S, bottom ash}$	$Y_{S, cyclone ash}$	$Y_{S, cooler ash}$	$Y_{S, filter ash}$
Air-fired	6.6	3.0	15.1	9.0
OF35	6.5	3.6	8.1 and 16.8	9.3
OF43w	6.8	3.7	12.4 and 17.9	9.9

Figure 4.23 shows the sulfur mass flows in the ashes based on the results presented in Figure 4.22 and Table 4.3. The error bars for the residual ashes indicate the variability of the sulfur mass fraction, as described above. The sulfur flow in the ash was higher in the oxy-fuel cases than in the air-fired case, due to the slightly higher average sulfur fraction in the ash and higher mass flows of the bottom and residual ashes in the oxy-fuel cases.

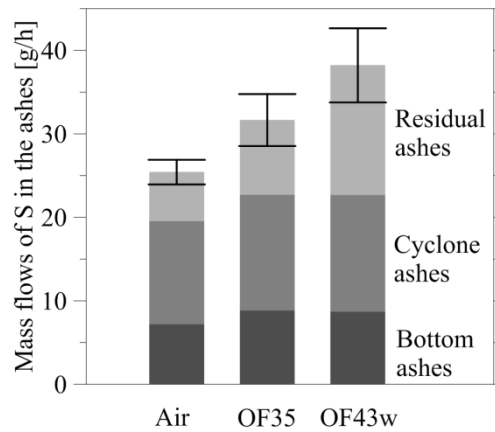


Figure 4.23 Resulting sulfur mass flows in the ash. An error bar is given for the residual ash, indicating the range of variability in the sulfur mass fraction (Paper II).

It was of interest to check whether a correlation exists between the concentration of sulfur in the ashes and the particle size of the ashes. Therefore, the particle size distribution of the ashes was determined for the bottom ash (Figure 4.24a) and cyclone ash (Figure 4.24b) from the OF43w case. The particle size distribution of the filter ash is shown in Figure 4.24c. The filter ash sample was taken after completion of all the test cases. The average particle size of the filter ash particles was, as expected, small compared to those of the other ashes. The size distribution of the particles in the bottom ash was broader than that of the cyclone ash.

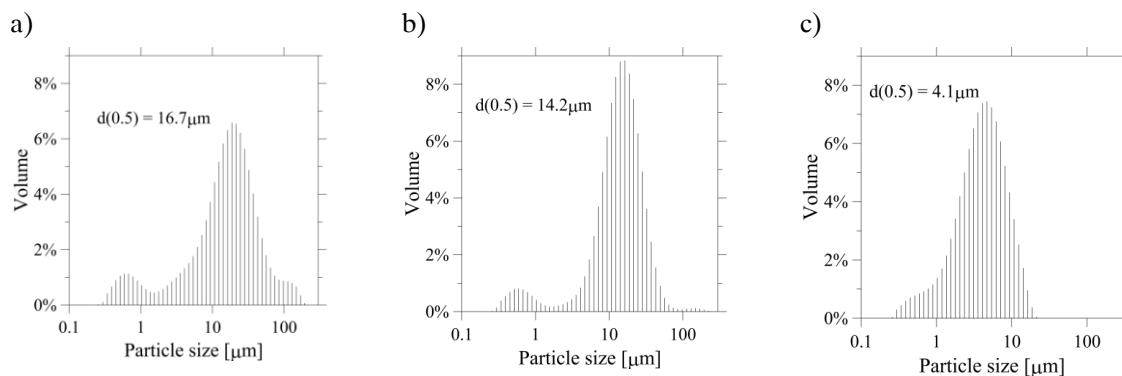


Figure 4.24 Particle size distribution in the: a) bottom ash from the OF43w case; b) cyclone ash from the OF43w case; and c) ash sample taken from the fabric filter (Paper II).

Smaller particles with a larger surface area per unit mass generally capture more SO_2 than larger particles, whereas the blockage of pores during CaSO_4 formation tends to inactivate more material than it is the case for smaller particles. Therefore, the reason for the larger sulfur fraction in the filter ash, as compared to the cyclone ash, is the smaller particle size of the filter ash. In addition, possible absorption of SO_3 by the filter ash would increase further the sulfur content of the filter ash, in comparison to the cyclone ash. The larger sulfur mass fraction in the bottom ash than in the cyclone ash can be explained by the fact

that the bottom ash was exposed to the flue gas during the entire experiment, whereas the cyclone ash was separated from the flue gas. The bottom ash in the furnace remained at a temperature that was suitable for the capture of SO₂.

Figure 4.25 gives the sulfur mass balance for the air-fired, OF35, and OF43w cases. The sulfur input from the fuel was set at 100%. The fraction of fuel sulfur found in the flue gas is equal to the conversion of fuel sulfur to SO₂ (presented in Figure 4.18). The sulfur found in the condensed water had only a minor influence on the mass balance. The error bars for the sulfur levels in the ash indicate the variations in levels of sulfur in the residual ashes. The sum of the estimated outlet sulfur flows was lower than the input sulfur flow by the fuel in all the test cases. The difference was 6% to 9% for the air-fired case, 21% to 27% for the OF35 case, and 8% to 17% for the OF43w case. Sulfur self-retention by the ash was higher in the oxy-fuel cases than in the air-fired case. The most likely reason for this is the increase in SO_x concentration during oxy-fuel combustion, which favors the formation of sulfates.

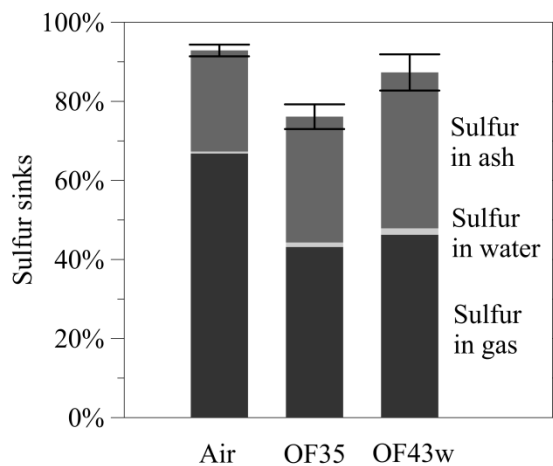


Figure 4.25 Sulfur sinks. The 100% level represents the sulfur introduced by the fuel, and the bars represent the sulfur sinks. An error bar is included, indicating the range of variation for the sulfur mass fraction (Paper II).

5 - Conclusions

The chemistry of sulfur under air-fired and oxy-fuel combustion conditions was investigated through experiments and modeling studies. The experimental work was carried out in the Chalmers 100-kW_{th} oxy-fuel unit with coal and propane as the fuels. Additional experiments were performed with a quartz reactor at the University of Zaragoza. The formation and measurement of SO₃/H₂SO₄ were of special interest in the present work. The modeling work was based on a detailed chemical reaction scheme with the focus on gas-phase reactions. The data processing was performed with the CHEMKIN-PRO software.

Investigations of the gas-phase chemistry indicate that the SO₃ concentration increases in line with the concentrations of O₂, H₂O, and CO₂ in the absence of combustibles. At temperatures <1000 K, SO₃ formation is insignificant. In the presence of combustibles, SO₃ formation is strongly increased for experimental temperatures between 1100 K and 1300 K, and H₂O and CO₂ have inhibitory effects on SO₃ formation. It was found that the concentration of SO₃ in the flue gas under oxy-fuel conditions tended to be several times higher than in air-fired combustion. The main reason for this is the higher concentration of SO₂ during oxy-fuel combustion.

The study of different SO₃ measurement techniques shows that the controlled condensation method and the salt method are suitable for SO₃ measurements. The Pentol SO₃ monitor is recommended if long-term continuous SO₃ measurements are of interest. The isopropanol absorption bottle method and the acid dew-point meter are not recommended for measuring SO₃ in flue gases.

In the experiments performed in the Chalmers oxy-fuel unit with lignite as the fuel, the SO₂ emissions were around 35% lower during oxy-fuel combustion than during air-fired combustion, although the concentration of SO₂ was more than three-times higher in the oxy-fuel combustion due to the lower total gas flow. These experiments demonstrate increased sulfur self-retention of the ash during oxy-fuel combustion, as compared to air-fired combustion, possibly as a result of the higher concentration of SO₂.

While it is advantageous that oxy-coal combustion leads to reduced SO₂ emissions, a higher concentration of SO₃ can be expected. This is mainly due to

the increased concentration of SO_2 in oxy-coal combustion, which leads to a greater risk of high- and low-temperature corrosion in oxy-coal combustion. The increased concentration of SO_3 increases the acid dew-point temperature, especially if a wet recycle is applied, since an increase in the H_2O concentration increases further the acid dew-point temperature. The CO_2 atmosphere in oxy-fuel combustion can, depending on the conditions, both favor and reduce the formation of SO_3 . It is difficult to generalize as what will happen in an oxy-fuel power plant. However, it is likely that the level of SO_3 formation in an oxy-fuel power plant is more affected by changes in the temperature-time history and FGR conditions than by the changed atmosphere itself, as shown in the present work. The formation of SO_3 is enhanced for a reduced FGR ratio by: 1) increased furnace temperature; 2) prolonged furnace residence time; and 3) increased concentration of O_2 in the feed gas.

6 - References

1. Corey, R. C.; Cross, B. J.; Reid, W. T. External Corrosion of Furnace-Wall Tubes – II Significance of Sulphate Deposits and Sulphur Trioxide in Corrosion Mechanism. *Trans. ASME* **1945**, 67, 289-302.
2. Otsuka, N. Effects of fuel impurities on the fireside corrosion of boiler tubes in advanced power generating systems – a thermodynamic calculation of deposit chemistry. *Corrosion Science* **2002**, 44, 265-283.
3. Nelson, W.; Cain, C. Corrosion of Superheaters and Reheaters of Pulverized-Coal-Fired Boilers. *Trans. ASME* **1960**, 82, 194-204.
4. Harb, J. N.; Smith, E. E. Fireside corrosion in PC-fired boilers. *Prog. Energy Combust. Sci.* **1990**, 16, 169-190.
5. Davis, C. Impact of Oxyfuel Operation on Corrosion in Coal Fired Boilers based on Experience with E.ON's 1MW_{th} Combustion Test Facility. *IEAGHG Special Workshop on Oxyfuel Combustion 25th – 26th January 2011*, London.
6. Francis, W. E. The measurement of the dewpoint and H₂SO₄ vapour content of combustion products. *Gas Research Board Communication* **1952**, 64, 1-37.
7. Hardman, R.; Stacy, R. Estimating Sulfuric Acid Aerosol Emissions from Coal-Fired Power Plants. *Conference on Formation, Distribution, Impact, and Fate of Sulfur Trioxide in Utility Flue-gas Streams*, Pittsburgh **1998**, 1-11.
8. Land, T. Theory of acid deposition and its application to the dew-point meter. *J. Inst. Fuel* **1977**, 50, 68-75.
9. Fleig, D.; Normann, F.; Andersson, K.; Johnsson, F.; Leckner, B. The fate of sulphur during oxy-fuel combustion of lignite. *Energy Procedia* **2009**, 1, 383-390.
10. Piper, J. D.; van Vliet, H. Effect of Temperature Variation on Composition, Fouling Tendency, and Corrosiveness of Combustion Gas from a Pulverized-Fuel-Fired Steam Generator. *Trans. ASME* **1958**, 80, 1251-1263.

11. Huijbregts, W. M. M.; Leferink, R. Latest advances in the understanding of acid dewpoint corrosion: corrosion and stress corrosion cracking in combustion gas condensates. *Anti-Corrosion Methods and Materials* **2004**, 51, 173-188.
12. Verhoff, F. H.; Choi, M. K. Effects of sulphuric acid condensation on stack equipment. *J. Inst. Energy* **1980**, 92, 92-99.
13. Dahl, L. Corrosion in flue-gas desulfurization plants and other low temperature equipment. *Werkstoffe und Korrosion* **1992**, 43, 298-304.
14. Srivastava, R. K.; Miller, C. A.; Erickson, C.; Jambhekar, R. Emissions of Sulfur Trioxide from Coal-Fired Power Plants. *POWER-GEN International* **2002**.
15. Moser, R. E. SO₃'s impacts on plant O&M: Part I. *Power* **2006**, 150, 40-42.
16. Matsuda, S.; Kamo, T.; Kato, A.; Nakajima, F.; Kumura, T.; Kuroda, H. Deposition of Ammonium Bisulfate in the Selective Catalytic Reduction of Nitrogen Oxides with Ammonia. *Ind. Eng. Chem. Prod. Res. Dev.* **1982**, 21, 48-52.
17. Verhoff, F. H.; Banchemo, J. T. Predicting Dew Points of Flue-gases. *Chem. Eng. Prog.* **1974**, 70, 71-72.
18. Marten, J. C. A history of flue gas desulfurization systems since 1850. *Journal of the Air Pollution Control Association* **1977**, 27, 948-960.
19. Smith, S. J.; van Aardenne, J.; Klimont, Z.; Andres, R. J.; Volke, A.; Delgado Arias, S. Anthropogenic sulfur dioxide emissions: 1850-2005. *Atmos. Chem. Phys.* **2011**, 11, 1101-1116.
20. Adams, B.; Senior, C. Curbing the blue plume: SO₃ formation and mitigation. *Power*, **2006**, 150, 39-42.
21. Jones, C.; Ellison, W. SO₃ tinges stack gas from scrubbed coal-fired units. *Power* **1998**, 142, 73-75.
22. Raask, E. Sulphate capture in ash and boiler deposits in relation to SO₂ emission. *Prog. Energy Combust. Sci.* **1982**, 8, 261-276.
23. Attar, A. Chemistry, thermodynamics and kinetics of reactions of sulfur in coal-gas reactions: a review. *Fuel* **1978**, 57, 201-212.
24. Adolphi, P.; Störr, M.; Mahlberg, P. G.; Murray, H. H.; Ripley, E. M. Sulfur sources and sulfur bonding of some central European attrital brown coals. *Int. J. Coal Geol.* **1990**, 16, 185-188.

25. Manovic, V.; Grubor, B.; Repic, B.; Mladenovic, M.; Jovanovic, M. Sulfur release during combustion of Serbian coals. *Fresenius Environ. Bull.* **2003**, *12*, 1348-1353.
26. Halstead, W. D.; Raask, E. The behaviour of sulphur and chlorine compounds in pulverized-coal-fired boilers. *J. Inst. Fuel* **1969**, *42*, 344-349.
27. Durie, R. A.; Matthews, C. J.; Smith, M. Y. The Catalytic Formation of Sulfur Trioxide in Fuel-Rich Propane-Air Flames. *Combust. Flame* **1970**, *15*, 157-165.
28. Schofield, K. The Kinetic Nature of Sulfur's Chemistry in Flames. *Combust. Flame* **2001**, *124*, 137-155.
29. Rees, O. W.; Shimp, N. F.; Beeler, C. W.; Kuhn, J. K.; Helfinstine, R. J. Sulfur retention in bituminous coal ash. *Circ.-Ill. State Geol. Surv.* **1966**, *396*, 1-10.
30. Sheng, C.; Xu, M.; Zhang, J.; Xu, Y. Comparison of sulphur retention by coal ash in different types of combustors. *Fuel Process. Technol.* **2000**, *64*, 1-11.
31. Osborn, G. A. Review of sulfur and chlorine retention in coal-fired boilers deposits. *Fuel* **1992**, *71*, 131-142.
32. Grubor, B.; Manovic V. Influence of Non-Uniformity of Coal and Distribution of Active Calcium on Sulfur Self-Retention by Ash – A Case Study of Lignite Kolubara. *Energy Fuels* **2002**, *16*, 951-955.
33. Cooper, B. R.; Ellingson, W. A. *The Science and Technology of Coal and Coal Utilization*; Plenum Press: New York, **1984**; pp 21-25.
34. Fleig, D.; Andersson, K.; Johnsson, F.; Leckner, B. Conversion of Sulfur during Pulverized Oxy-coal Combustion. *Energy Fuels* **2011**, *25*, 647-655.
35. Woycenko, D.; Ikeda, I.; van de Kamp, W. L. Combustion of pulverized coal in a mixture of oxygen and recycled flue-gas. *Technical Report IFRF (International Flame Research Foundation) Doc F98/Y/1*, IJmuiden **1994**.
36. Croiset, E.; Thambimuthu, K. V. NO_x and SO₂ emissions from O₂/CO₂ recycle coal combustion. *Fuel* **2001**, *80*, 2117-2121.
37. Kiga, T.; Takano, S.; Kimura, N.; Omata, K.; Okawa, M.; Mori, T.; Kato, M. Characteristics of pulverized-coal combustion in the system of oxygen/recycled flue-gas combustion. *Energy Convers. Mgmt* **1997**, *38*, 129-134.

38. Mönckert, P.; Dhungel, B.; Kull, R.; Maier, J. Impact of Combustion Conditions on Emission Formation (SO₂, NO_x) and fly ash, *3th Workshop IEAGHG Int. Oxy-Combustion Network*, Yokohama **2008**.
39. Tan, Y.; Croiset, E.; Douglas, M. A.; Thambimuthu, K. V. Combustion characteristics of coal in a mixture of oxygen and recycled flue-gas. *Fuel* **2006**, 85, 507-512.
40. Stanger, R.; Wall, T. Sulphur impacts during pulverised coal combustion in oxy-fuel technology for carbon capture and storage. *Prog. Energy Combust. Sci.* **2011**, 37, 69-88.
41. Abele, A. R.; Kindt, G. S.; Clark, W. D.; Payne, R.; Chen, S. L. An experimental program to test the feasibility of obtaining normal performance from combustors using oxygen and recycled gas instead of air. *Argonne National Laboratory Report ANL/CNSV-TM-204*, Irvine **1987**.
42. Cheng, J.; Zhou, J.; Liu, J.; Zhou, Z.; Huang, Z.; Cao, X.; Zhao X.; Cen, K. Sulfur removal at high temperatures during coal combustion in furnaces: a review. *Prog. Energy Combust. Sci.* **2003**, 29, 381-405.
43. Liu, H.; Okazaki, K. Simultaneously easy CO₂ recovery and drastic reduction of SO_x and NO_x in O₂/CO₂ coal combustion with heat recirculation. *Fuel* **2003**, 82, 1427-1436.
44. Liu, H.; Katagiri, S.; Okazaki, K. Drastic SO_x removal and influences of various factors in O₂/CO₂ pulverized coal combustion system. *Energy Fuels* **2001**, 15, 403-412.
45. Chen, C.; Zhao, C. Mechanism of Highly Efficient In-Furnace Desulfurization by Limestone under O₂/CO₂ Coal Combustion Atmosphere. *Ind. Eng. Chem. Res.* **2006**, 45, 5078-5085.
46. Chen, C.; Zhao, C.; Liang, C.; Pang, K. Calcination and sintering characteristics of limestone under O₂/CO₂ combustion atmosphere. *Fuel Process. Technol.* **2007**, 88, 171-178.
47. Wang, C.; Jia, L.; Tan, Y.; Anthony, E. J. Carbonation of fly ash in oxy-fuel CFB combustion. *Fuel* **2008**, 87, 1108-1114.
48. Yrjas, P.; Iisa, K.; Hupa, M. Comparison of SO₂ capture capacities of limestones and dolomites under pressure, *Fuel* **1995**, 74, 395-400.
49. Hindiyarti, L.; Glarborg, P.; Marshall, P. Reactions of SO₃ with the O/H Radical Pool under Combustion Conditions. *J. Phys. Chem.* **2007**, 111, 3984-3991.

50. Fernando, R. SO₃ issues for coal-fired plant. *IEA Clean Coal Centre* **2003**, PF 03-03, 1-53.
51. Reidick, H.; Reifenhäuser, R. Katalytische SO₃ –Bildung in Abhängigkeit von der Kesselverschmutzung. *VGB Kraftwerkstechnik* **1978**, 58, 915-921.
52. Maier, P.; Dibbs, H. P. The catalytic conversion of SO₂ to SO₃ by fly ash and the capture of SO₂ and SO₃ by CaO and MgO. *Thermochim. Acta* **1974**, 8, 155-165.
53. Wickert, K. Die katalytische SO₂-Oxydation in Abhängigkeit von der Verweilzeit der Gase im Reaktionsraum. *BWK* **1962**, 14, 20-21.
54. Jørgensen, T. L.; Livbjerg, H.; Glarborg, P. Homogeneous and heterogeneously catalyzed oxidation of SO₂. *Chem. Eng. Sci.* **2007**, 62, 4496-4499.
55. Urbanek, A.; Trela, M. Catalytic Oxidation of Sulfur Dioxide. *Catal. Rev. Sci. Eng.* **1980**, 21, 73-133.
56. Armitage, J. W.; Cullis, C. F. Studies of the Reaction Between Nitrogen Dioxide and Sulfur Dioxide. *Combust. Flame* **1971**, 16, 125-130.
57. Wendt, J. O. L.; Sternling, C. V. Catalysis of SO₂ Oxidation by Nitrogen Oxides. *Combust. Flame* **1973**, 21, 387-390.
58. Glarborg, P. Hidden interactions – Trace species governing combustion and emissions. *Proceedings of the Combustion Institute* **2007**, 31, 77-98.
59. Couling, D. Impact of Oxyfuel Operation on Emissions and Ash Properties based on E.ON's 1MW CTF. *IEAGHG Special Workshop on Oxyfuel Combustion*, London 25th – 26th January **2011**.
60. Kenney, J. R.; Clark, M. M.; Levasseur, A. A.; Kang, S. G. SO₃ Emissions from a Tangentially-Fired Pilot Scale Boiler Operating under Oxy-Combustion Conditions. *IEAGHG Special Workshop on Oxyfuel Combustion*, London 25th – 26th January **2011**.
61. Eddings, E. G.; Ahn, J.; Okerlund, R.; Fry, A. SO₃ Measurements under Oxy-Coal Conditions in Pilot-Scale PC and CFB Combustors. *IEAGHG Special Workshop on Oxyfuel Combustion*, London 25th – 26th January **2011**.
62. Liu, F.; Guo, H.; Smallwood, G. J.; Gülder, Ö. L. The Chemical Effects of Carbon Dioxide as an Additive in an Ethylene Diffusion Flame: Implications for Soot and NO_x Formation. *Combust. Flame* **2001**, 125, 778-787.

63. Glarborg, P.; Bentzen, L. L. B. Chemical Effects of a High CO₂ Concentration in Oxy-Fuel Combustion of Methane. *Energy Fuels* **2008**, *22*, 291-296.
64. Cooper, D. Optimisation of a NaCl Adsorbent Tube Method for SO₃ Measurements in Combustion Flue Gases. *Institutet för Vatten- och Luftvårdsforskning (IVL) Göteborg*, **1995**, Report B-1177.
65. Cooper, D.; Andersson, C. (in Swedish) Bestämning av SO₃ i rökgaser med NaCl-metoden – en jämförelse av olika metoder. *Värmeforsk and Institutet för Vatten- och Luftvårdsforskning (IVL) Göteborg* **1997**, Värmeforsk report 616.
66. Cooper, D.; Ferm, M. Jämförelse av mätmetoder för bestämning av SO₃-koncentrationer i rökgaser. *Värmeforsk and Institutet för Vatten- och Luftvårdsforskning (IVL) Göteborg*, **1994**, Värmeforsk report 494.
67. Cao, Y.; Zhou, H.; Jiang, W.; Chen, C.; Pan, W. Studies on the fate of sulfur trioxide in coal-fired utility boilers based on modified selected condensation methods. *Environ. Sci. Technol.* **2010**, *44*, 3429-3434.
68. Dene, C.; Himes, R. Continuous Measurement Technologies for SO₃ and H₂SO₄ in Coal-Fired Power Plants. Technical report *EPRI (Electric Power Research Institute)*, Palo Alto **2004**.
69. Kel'man, F. N., (in Russian) *Zavodskaya Lab.* **1952**, *11*, 1316-1318.
70. Roiter, V. A.; Stukanovskaya, N. A.; Korneichuk, G. P.; Volikovskaya; Golodets, G. I. *Translation from Kinetika i Kataliz* **1960**, *1*, 408-417.
71. Pentol-Enviro AG, *SO₃ Monitor*, Basel, Switzerland, Available from: <http://www.pentol.net>.
72. Blauenstein, O. Personal communication with respect to SO₃ measurements, Mail: olivier.blauenstein@pentol.net, Phone: +497624300130, Pentol GmbH, Degussaweg 1, D-79639 Grenzach-Wyhlen, **2008**.
73. Jackson, P. J.; Hilton, D. A.; Buddery, J. H. Continuous measurement of sulfuric acid vapour in combustion gases using a portable automatic monitor. *J. Inst. Energy* **1981**, 124-135.
74. Gustavsson, L.; Nyquist, G. *Värmeforsks Mäthandbok. Värmeforsk Service AB utgåva 3*, Stockholm **2005**.
75. Maddalone, R. F.; Newton, S. F.; Rhudy, R. G.; Statnick, R. M. Laboratory and field evaluation of the controlled condensation system for SO₃

- measurements in flue gas streams. *J. of the Air Pollution Control Association* **1979**, 29, 626-631.
76. Koebel, M.; Elsener, M. Schwefeltrioxidbestimmung in Abgasen nach der Isopropanolmethode – Eine kritische Betrachtung. *Gefahrstoffe – Reinhaltung der Luft* **1997**, 57, 193-199.
77. Installation and operation manual of Brooks® smart-series digital mass flow meters and controllers. **2003**, Appendix A page 28.
78. Stuart, D. D. Continuous Measurements of Acid Dewpoint and Sulfur Trioxide in Stack Gases. *101st Air and Waste Management Association annual conference and exhibition*, Portland 24th – 27th June, **2008**.
79. Johnstone, H. F. *University of Illinois*, **1929**, Circular No. 20, 1-22.
80. Taylor, A. A. *J. Inst. Fuel* **1942**, 16, 25-28.
81. LAND Instruments International, Dronfield S18 1DJ, England, <http://www.landinst.com/>.
82. Andersson, K.; Normann, F.; Johnsson, F.; Leckner, B. Nitrogen oxide emission during oxy-fuel combustion of lignite. *Ind. Eng. Chem. Res.* **2008**, 47, 1835-1845.
83. Senior, C. L.; Sarofim, A. F.; Zeng, T.; Helble, J. J.; Mamani-Paco, R. Gas-phase transformations of mercury in coal-fired power plants. *Fuel Process. Technol.* **2000**, 63, 197-213.
84. Giménez-López, J.; Martínez, M.; Millera, A.; Bilbao, R.; Alzueta M. U. SO₂ effects on CO oxidation in a CO₂ atmosphere, characteristic of oxy-fuel conditions. *Combust. Flame* **2011**, 158, 48-56.
85. Alzueta, M. U.; Bilbao, R.; Glarborg, P. Inhibition and Sensitization of Fuel Oxidation by SO₂. *Combust. Flame* **2001**, 127, 2234-2251.
86. Chemkin-Pro. Release 15101. *Reaction Design*, San Diego.
87. Kuehnemuth, D.; Normann, F.; Andersson, K.; Johnsson, F.; Leckner, B. Reburning of Nitric Oxide in Oxy-Fuel Firing - The Influence of Combustion Conditions. *Energy Fuels* **2011**, 25, 624-631.
88. Flint, D.; Lindsay, A. W. Catalytic oxidation of sulphur dioxide on heated quartz surfaces. *Fuel* **1951**, 30, 288.

89. Abián, M.; Giménez-López, J.; Bilbao, R.; Alzueta, M. U. Effect of different concentration levels of CO₂ and H₂O on the oxidation of CO: experiments and modeling. *Proc. Combust. Inst.* **2011**, 33, 317-323.
90. Crumley, P. H.; Fletcher, A. W. The Formation of Sulphur Trioxide in Flue Gases. *J. Inst. Fuel* **1956**, 29, 322-327.
91. Bolsaitis, P.; Elliott, J. F. Thermodynamic Activities and Equilibrium Partial Pressures for Aqueous Sulfuric Acid Solutions. *J. Chem. Eng. Data* **1990**, 35, 69-85.
92. Kasbohm, J. Zur thermischen Schwefelfreisetzung aus Braunkohlen. *Universität Greifswald, Dissertation* **1988**.